Geophysical mapping and imaging of soil structures: basic overview

Stéphane Garambois

Landslide team, LGIT, Université Joseph Fourier

Suivi d'infiltration/irrigation — *Oliveraie en Italie*

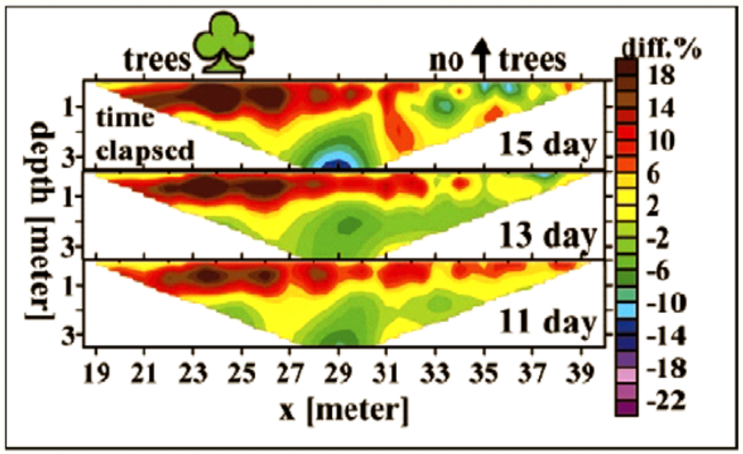

Figure 6. Differences of inverted resistivity models at Rio Frio showing an increase in dryness by root water uptake in the top 2 m within 15 days of monitoring. No irrigation.

3D imaging of the water table (seismic)

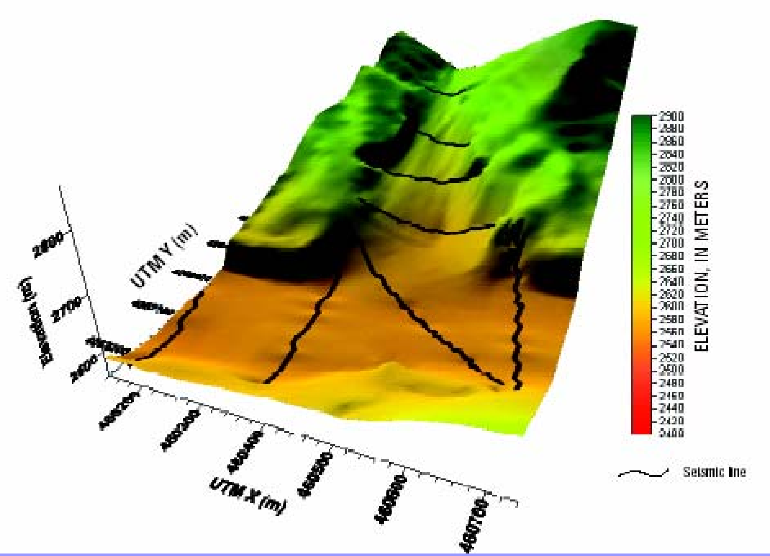

Plan

- 1- Introduction to environmental geophysics
- 2- Active potential methods

    2.1 Electrical

    2.2 Electromagnetics

- 3- Wave methods

    3.1 GPR (Ground Penetrating radar)

    3.2 Seismic

1. Environmental geophysics

Relatively new fields compares to oil and mine investigations

- Fast methods, low cost for preliminary investigations
- Large scale, 1D, 2D and 3D imaging, non intrusive, monitoring
- Necessity of independent calibrations (geotechnical, geochemical, …)
- Questions : Which method to use?
  - Sensitivity : chemico-physical parameter
  - Depth / Resolution
  - Price, time, scale
- Modern research : number of developments is increasing

Geophysical Methods are used to assist with many Hydrogeological Investigations, such as:
Mapping the Depth to Water Table and Bedrock
Fault Detection
Fresh/Salt Water Interface Mapping
Hydrostratigraphic/Lithologic Mapping
Landfill Delineation
Water Content Estimation
Fracture/Cavity Detection
Estimation of Hydraulic Parameters (porosity and permeability)
Water Quality Assessment
Assessing Integrity of Waste Containment Structures
Direct Detection of Contaminants
Monitoring Physio-Chemical-Microbiological Processes

Sensitivity to geophysical parameters

Propriétés physiques	Magnétisme	Gravimétrie	Electromag.	Electrique	Radar	Sismique
Succeptibilité k	P		S		S	
Densité d		P				S
Résistivité ohm.m			P	P	S	
Permittivité e			S		P	
Vitesse v						P

Figure 1-2 Propriétés physiques des roches et techniques géophysiques (P et S = effet prépondérant, respectivement secondaire sur la réponse géophysique)

How do geophysists see soil/rocks? porous media

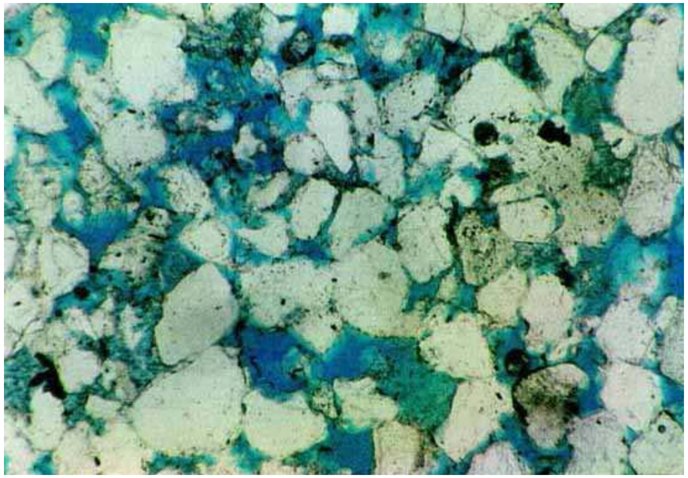

Grain matrix + Porosity + Fluids

(velocity, density, susceptibility, permittivity, conductivity, clays …)

Nature of the fluid, saturation, viscosity, salinity, presence of pollution, ….

Chemico-physical parameters of each of the phases

→ Physical parameters of the rocks/soil

I. 2 Classification of geophysical methods

Observation of a geophysical anomaly: 2D or 3D?

Profile

Mapping

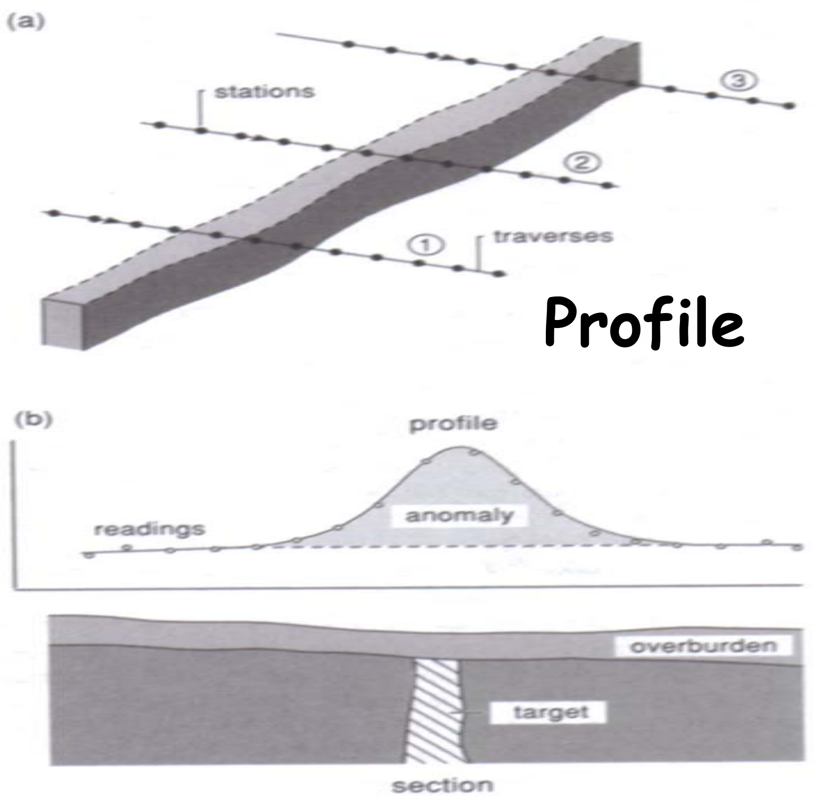

Figure 2.1 Traverses, stations, and profiles.

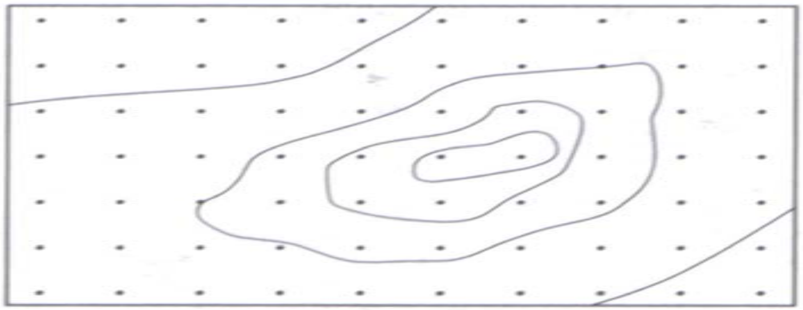

Figure 2.2 Grid of stations and contoured results.

Classification of geophysical methods

Images after inversion (tomography)

Images in reflexion mode (GPR, seismic)

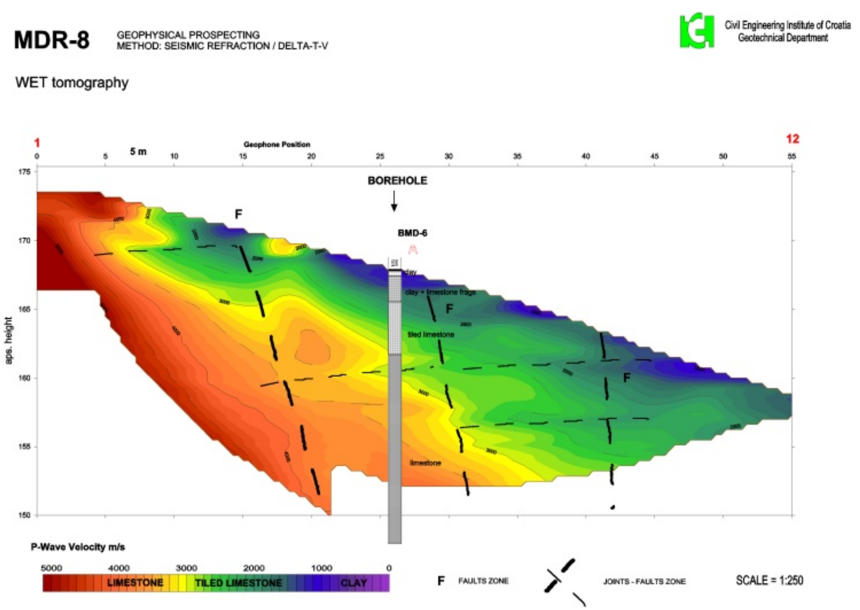

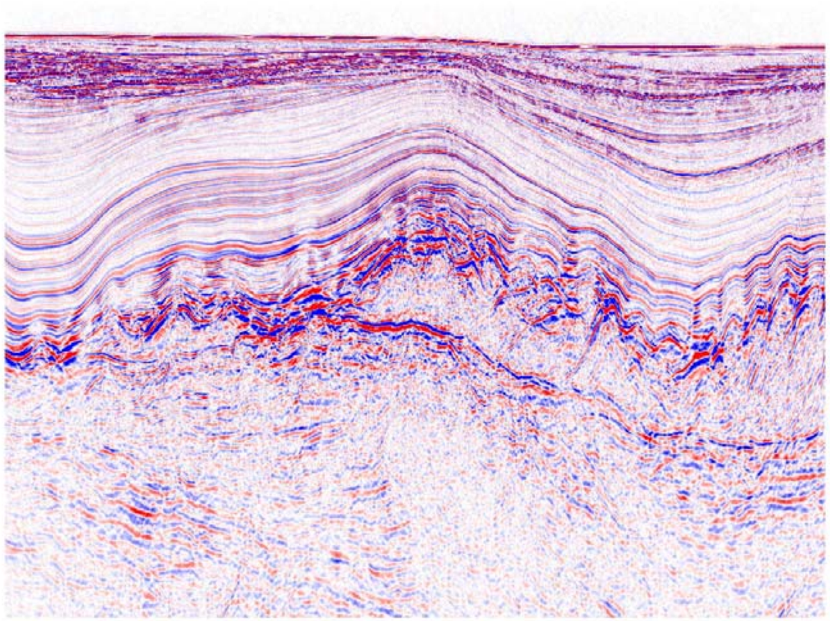

Characteristics of geophysical methods

Advantages

Light, nondestroying and varied techniques

- Important Volume of investigation
- Obtaining images in 2D and 3D

Limitations

Limitations

- **Methods require contrast in physical properties**
- **Nonuniqueness**

  Direct modeling: calculate the result of a specific structure

  Inverse modeling: determine the causative structure from observations – usually ambiguous

  e.g. small shallow body vs. large deep body
- **Resolution is determined by the wavelength of the signal**

  sesimic: km, radar: cm
- **Noise prevents recovery of low amplitude signal**

  e.g. wind, traffic, water pumps, power lines

2.1 Electrical methods

Comment ça marche? *Principe (loi d'Ohm)*

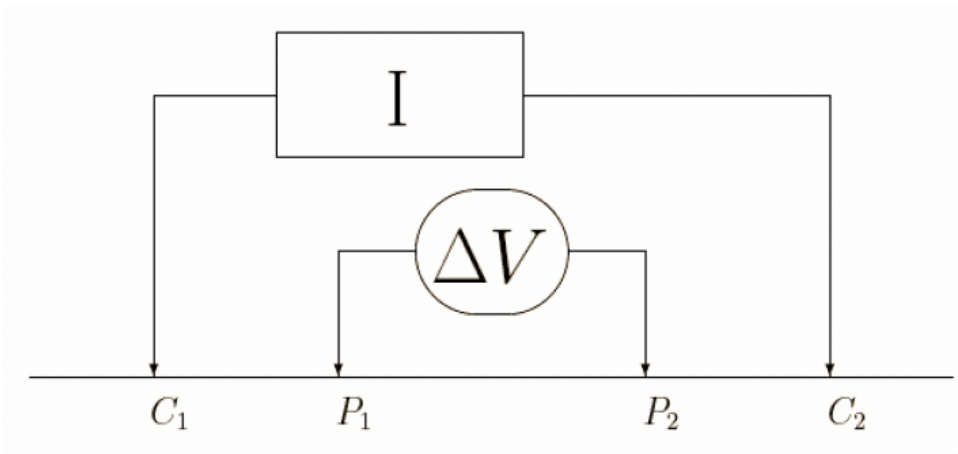

Loi d'Ohm :

$$\Delta V = RI$$

On utilise la résistivité ($\rho = RA/\ell$), d'où : $\frac{\Delta V}{\ell} = \frac{\rho I}{A}$, soit $-\nabla V = \rho \vec{j}$

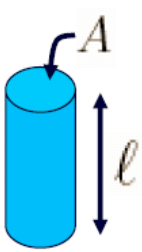

- R $[\Omega]$ est la résistance d'un circuit équivalent au volume du sous-sol traversé par le courant
- ρ $[\Omega.m^{-1}]$ est celle d'un élément de circuit de longueur ℓ et de section A

Sensitivity to resistivity to water (without clays)

Empirical law of Archie

$$\rho = a\,\phi^{-m} S^{-n} \rho_w \qquad (2.2)$$

ϕ : fractional pore volume (porosity)

S : fraction of the pores containing water

ρ_w: resistivity of water

$$n \approx 2$$

$$0.5 < a < 2.5$$

$$1.3 < m < 2.5$$

- There is considerable overlap between different rock types.
- Identification of a rock type is not possible solely on the basis of resistivity data.
- Resistivity of rocks depends on porosity, saturation, content of clay and resistivity of pore water (Archie's formula).

Resistivity values

Material	Resistivity (Ω•m)	Conductivity (Siemen/m)
Igneous and Metamorphic Rocks		
Granite	$5x10^{3}$ - 10^{6}	10^{-6} - $2x10^{-4}$
Basalt	10^{3} - 10^{6}	10^{-6} - 10^{-3}
Slate	$6x10^{2}$ - $4x10^{7}$	$2.5x10^{-8}$ - $1.7x10^{-3}$
Marble	10^{2} - $2.5x10^{8}$	$4x10^{-9}$ - 10^{-2}
Quartzite	10^{2} - $2x10^{8}$	$5x10^{-9}$ - 10^{-2}
Sedimentary Rocks		
Sandstone	8 - $4x10^{3}$	$2.5x10^{-4}$ - 0.125
Shale	20 - $2x10^{3}$	$5x10^{-4}$ - 0.05
Limestone	50 - $4x10^{2}$	$2.5x10^{-3}$ - 0.02
Soils and waters		
Clay	1 - 100	0.01 - 1
Alluvium	10 - 800	$1.25 x10^{-3}$ - 0.1
Groundwater (fresh)	10 - 100	0.01 - 0.1
Sea water	0.2	5
Chemicals		
Iron	$9.074x10^{-8}$	$1.102x10^{7}$
0.01 M Potassium chloride	0.708	1.413
0.01 M Sodium chloride	0.843	1.185
0.01 M acetic acid	6.13	0.163
Xylene	$6.998x10^{16}$	$1.429x10^{-17}$

Types d'eau	Concentration ppm	Résistivité ohms*m	Conductibilité microsiemens/cm
eau potable	500	12	833
eau médiocre	1000	6	1666
eau mauvaise	2000	2,8	3571
eau non potable	8000	0.75	13333
eau de mer	35000	0,2	50000
eau de Vichy	5167	1,2	8000
eau d'Henniez	500	12	833
eau du robinet	311	18	550

Figure 2-6 Résistivité de différents types d'eau

Type d'eau ou de polluant	Résistivité (ohm*m)
Eaux des rivières du plateau Suisse	15 – 35
Rhône	80
Lac Léman	40 – 50
Lac de Neuchâtel	40 – 50
Eau de pluie	30 – plusieurs milliers
Fleuve Balé (Mali)	300
Fleuve Niger	100
Hydrocarbure	Résistivité infinie
P :C :E. (Perchloréthylène)	Résistivité infinie
Jus de décharge	5

Figure 2-7 Résistivité de différentes eaux et de polluants

2.1 Electrical prospecting

- Apparent resistivity is measured on the field

-It results from the volume integration of all the soil cells crossed by the current lines as a function of the distance from the source

- If the soil is homogeneous, apparent resistivity=true resistivity

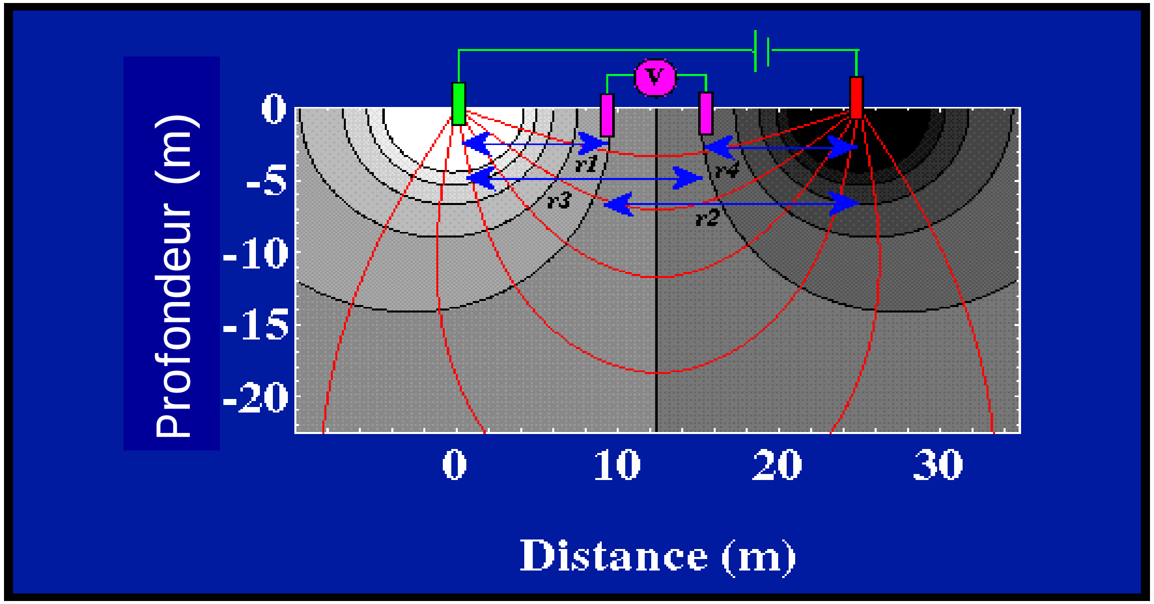

To measure the resistivity, we use a quadripole (dipoles of injection of current and of reception of the induced potential difference V

$$\rho_a = \frac{2\pi\Delta V}{i}\left[\frac{1}{\left(\frac{1}{r_1}-\frac{1}{r_2}-\frac{1}{r_3}+\frac{1}{r_4}\right)}\right]$$

Depth penetration as a function of injection electrodes spacing

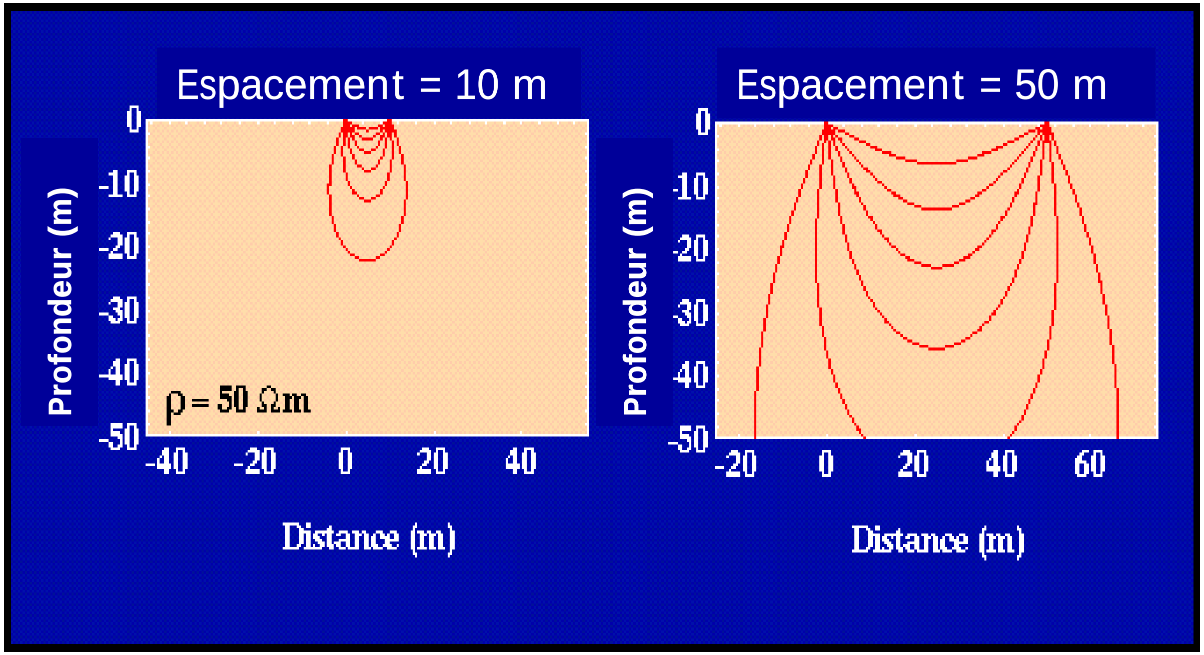

50 % of the total injected current flows on a depth lower than electrode spacing. To increase penetration, we increase electrode spacing.

Measurement configuration : profiling

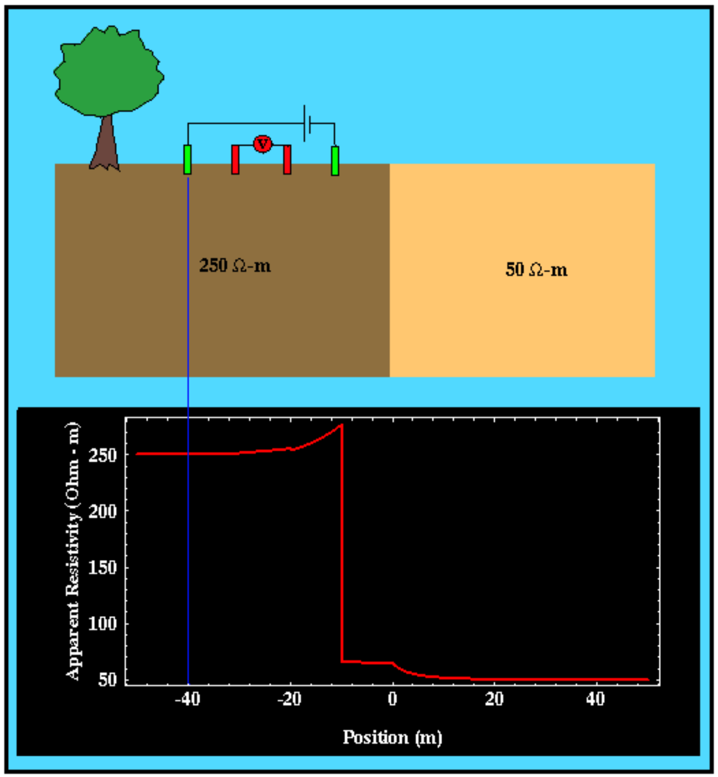

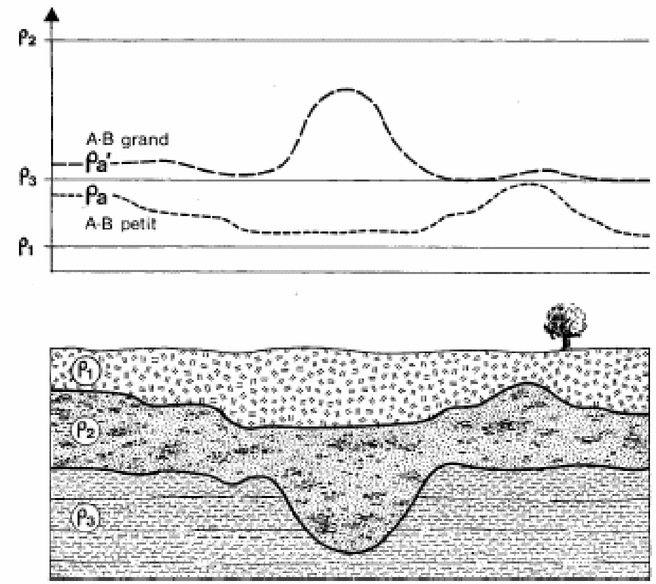

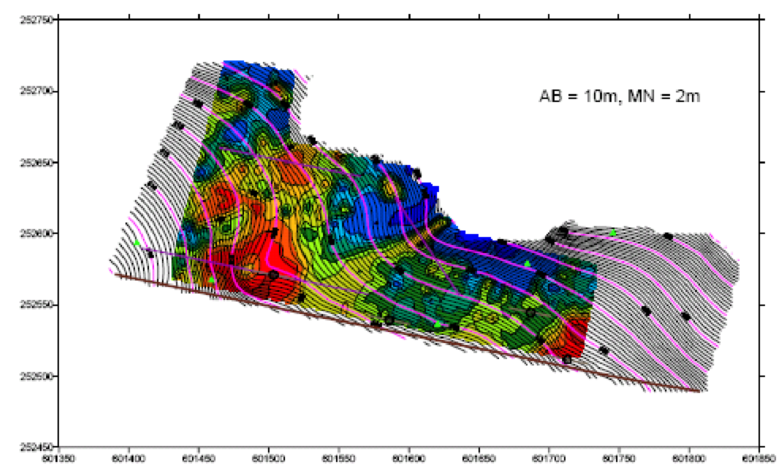

Figure 4-41 Exemple de carte de résistivités apparentes (Bâle 1999, AB = 10m) en milieu karstique. Les faibles résistivités font apparaître différentes directions d'écoulement invisibles en surface.

Measurement method : sounding

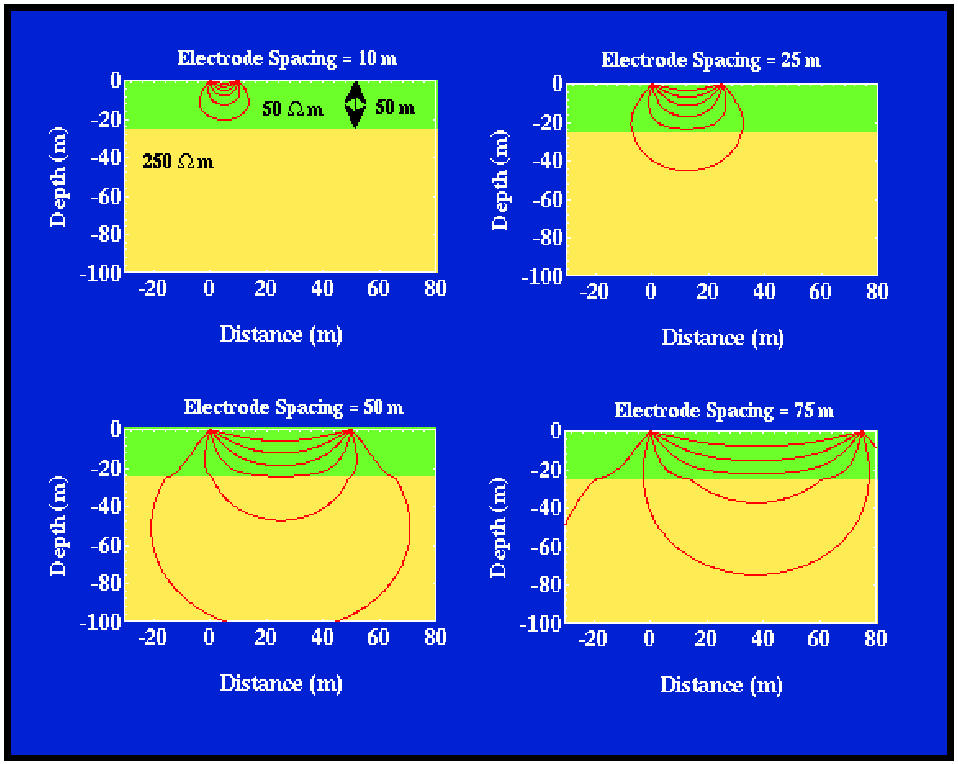

Cours de géophysique – Résistivités électriques – D. Chapellier – 2000/01

L'interprétation des sondages électriques multicouches peut être faite à partir d'un jeu d'abaques ou encore par ordinateur (Figure 6-56). Dans ce dernier cas, le géophysicien entre un modèle tenant compte des a priori géologiques et l'ordinateur calcule la réponse du modèle. Le géophysicien modifie alors le modèle de manière à ce que la courbe calculée corresponde aux mesures de terrain.

ÉTUDE MALI — M. Meyer **SONDAGE N° 2**

	Résistivité (ohms·m)	Epaisseur (m)	Profondeur (m)	
A	600	6,0	0,0	Altérites sableuses
	20	30,0	6,0	Altérites argileuses
	1000		36,0	Socle

	Résistivité (ohms·m)	Epaisseur (m)	Profondeur (m)	
B	600	6,0	0,0	Arènes d'altération
	20	26,0	6,0	Socle altéré
	200	3,0	32,0	Socle
	400	5,0	35,0	

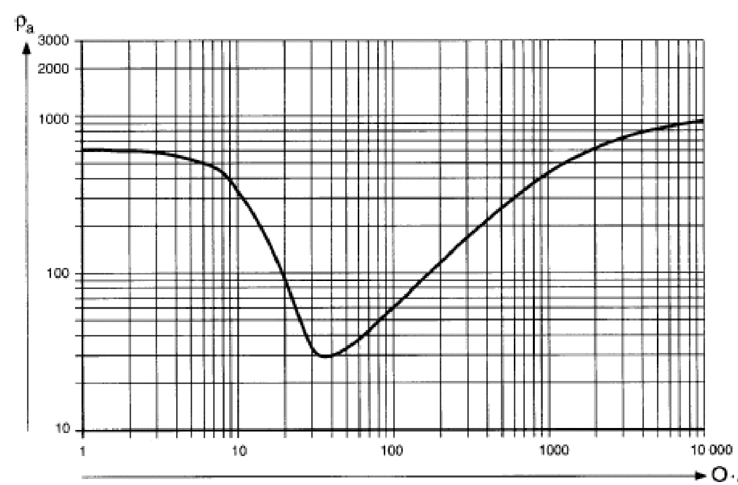

Figure 6-54 Exemple de suppression sur un sondage réel

Measurements method:electrical tomography

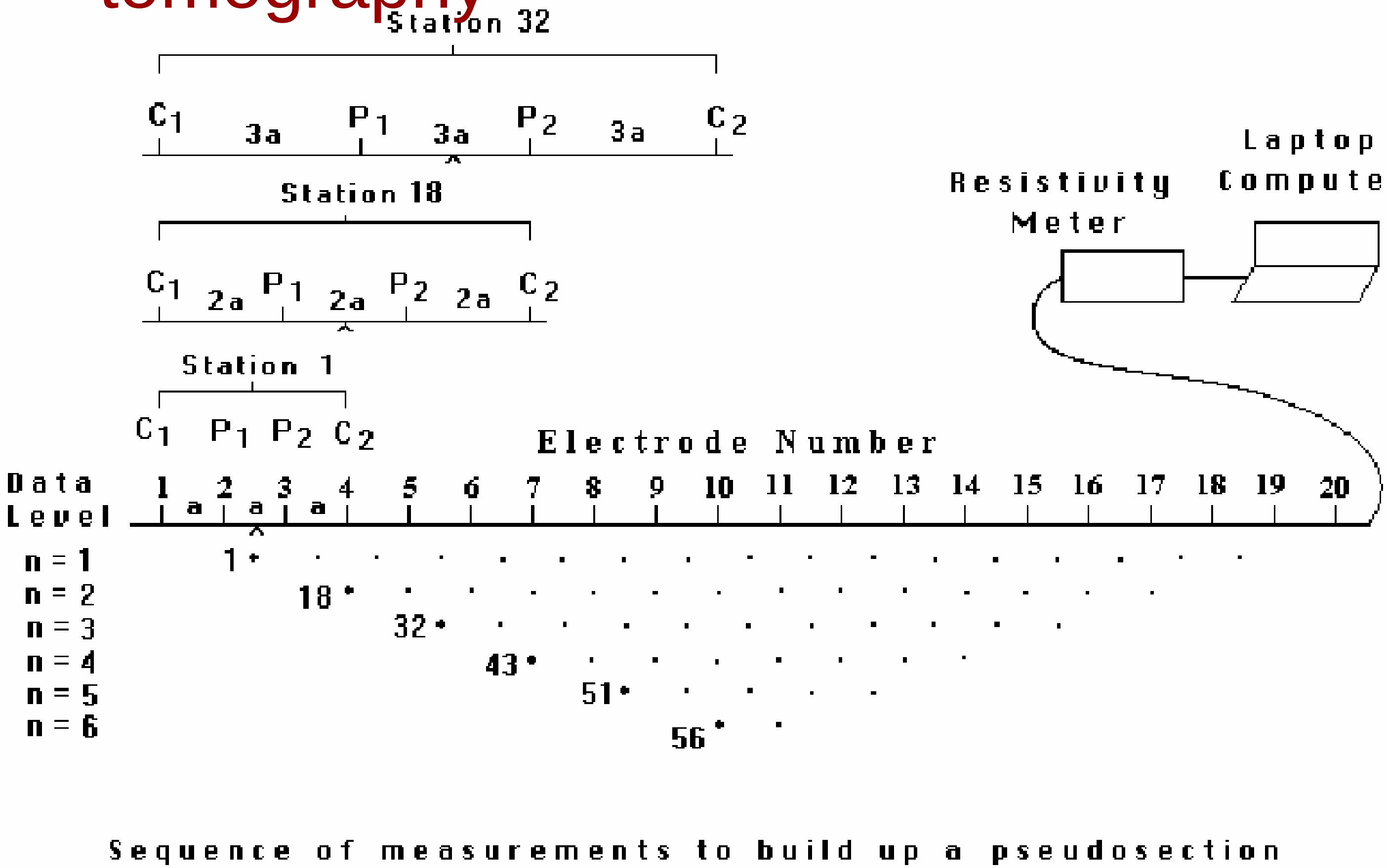

Figure 5. The arrangement of electrodes for a 2-D electrical survey and the sequence of measurements used to build up a pseudosection.

Application :waste site

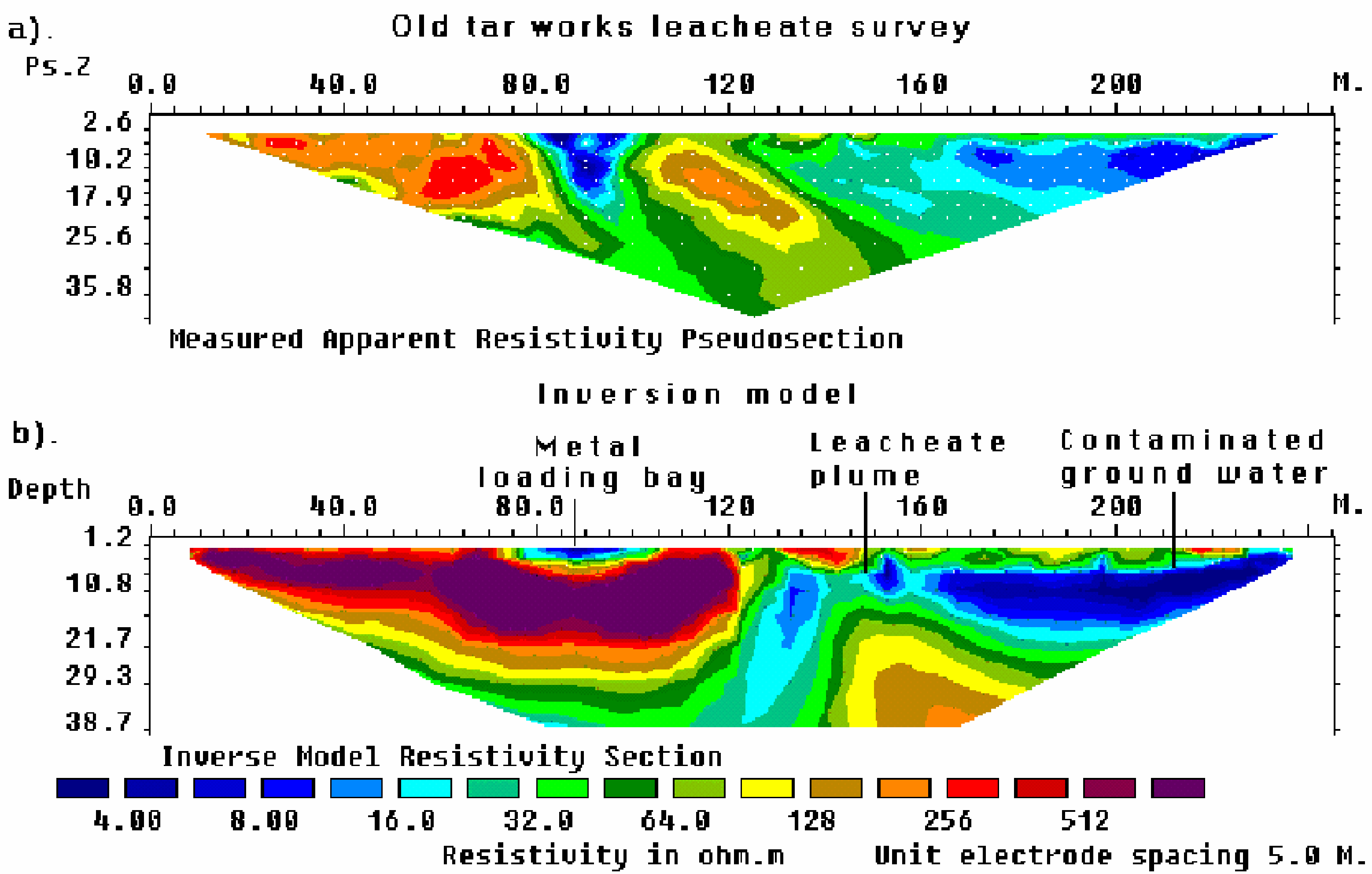

Figure 20. (a) The apparent resistivity pseudosection from a survey over a derelict industrial site, and the (b) computer model for the subsurface.

Agricultural site : nitrates

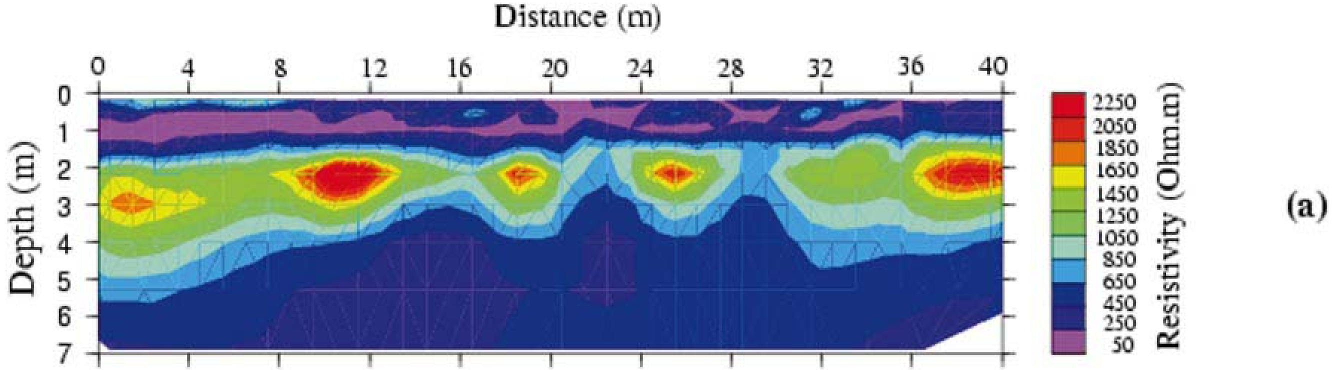

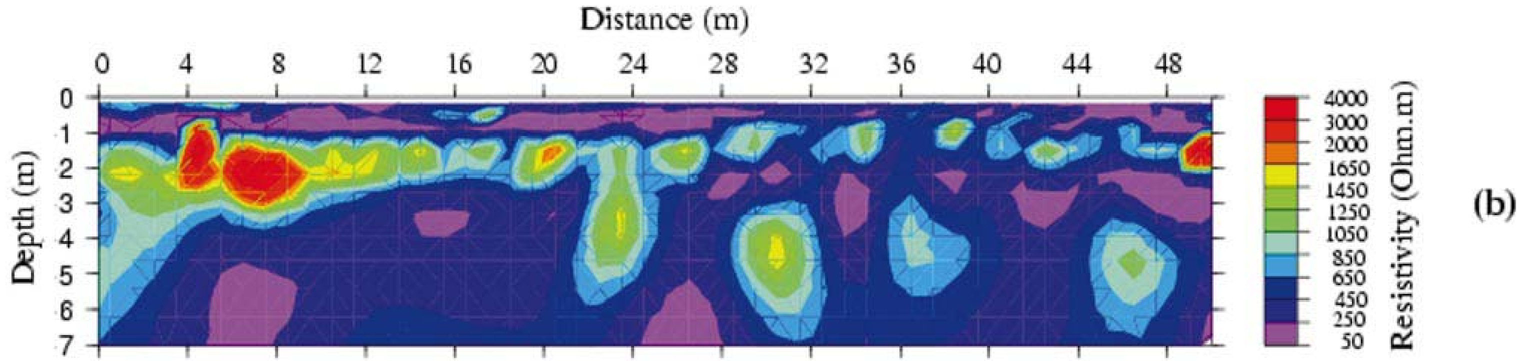

Peat bog of Chirens

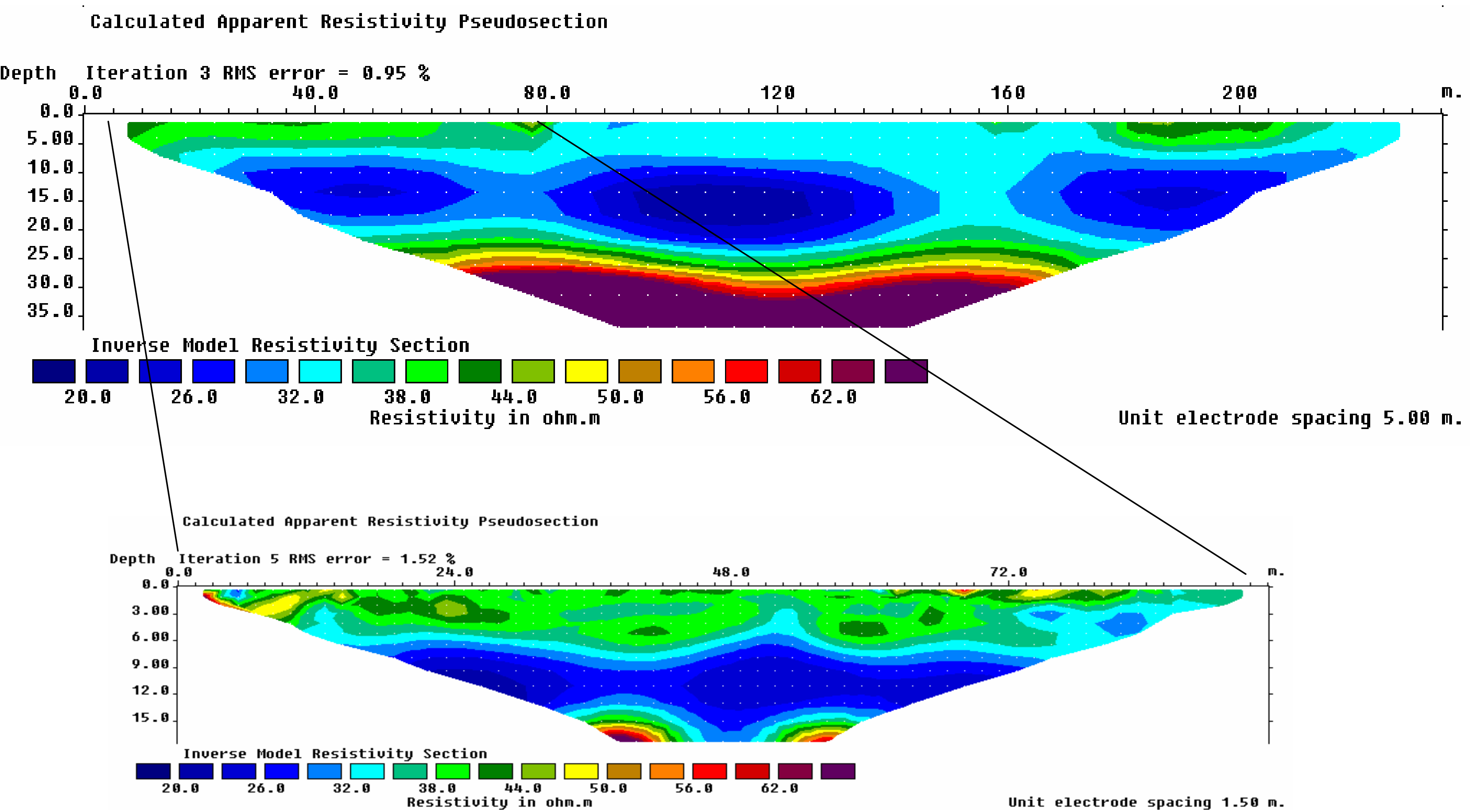

Water infiltration monitoring

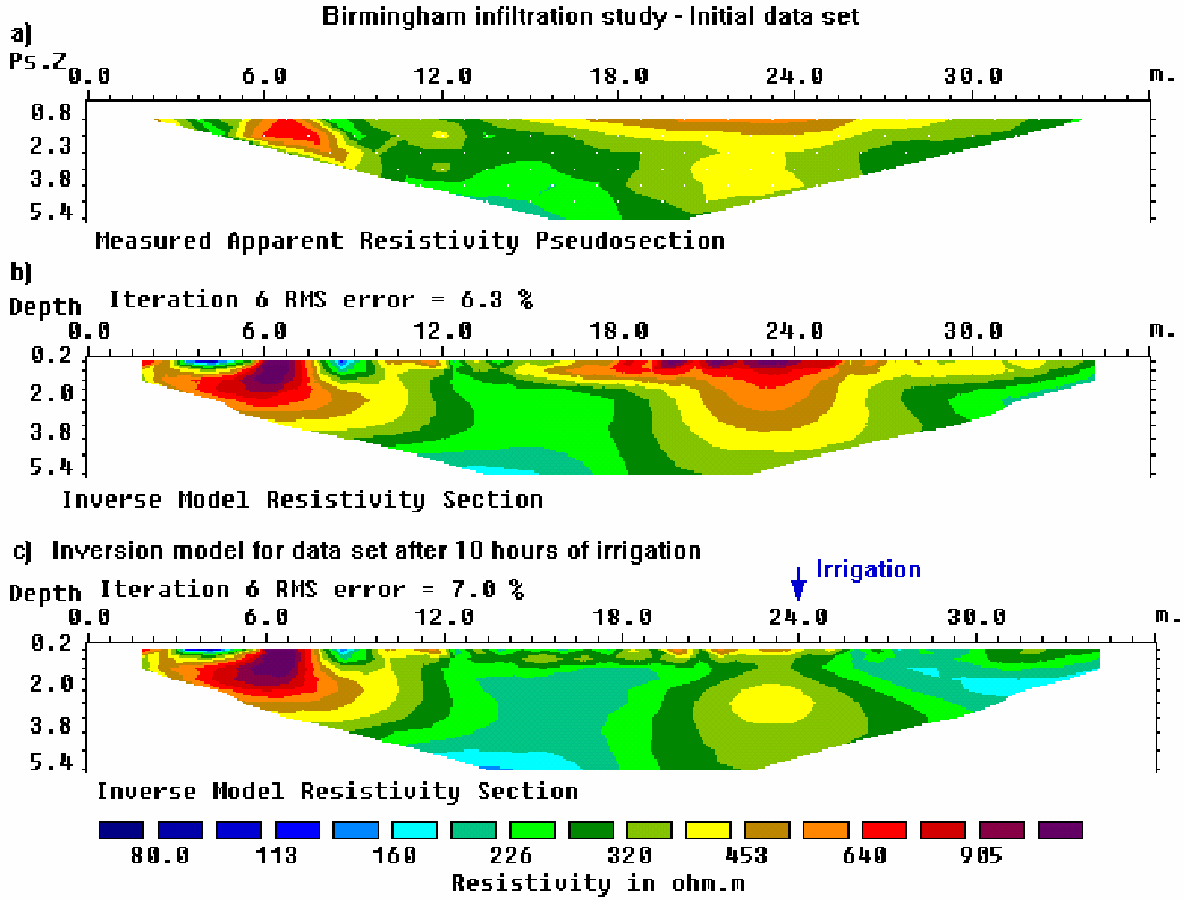

Figure 24. (a) The apparent resistivity and (b) inversion model sections from the survey conducted at the beginning of the Birmingham infiltration study. This shows the results from the initial data set that forms the base model in the joint inversion with the later time data sets. As a comparison, the model obtained from the inversion of the data set collected after 10 hours of irrigation is shown in (c).

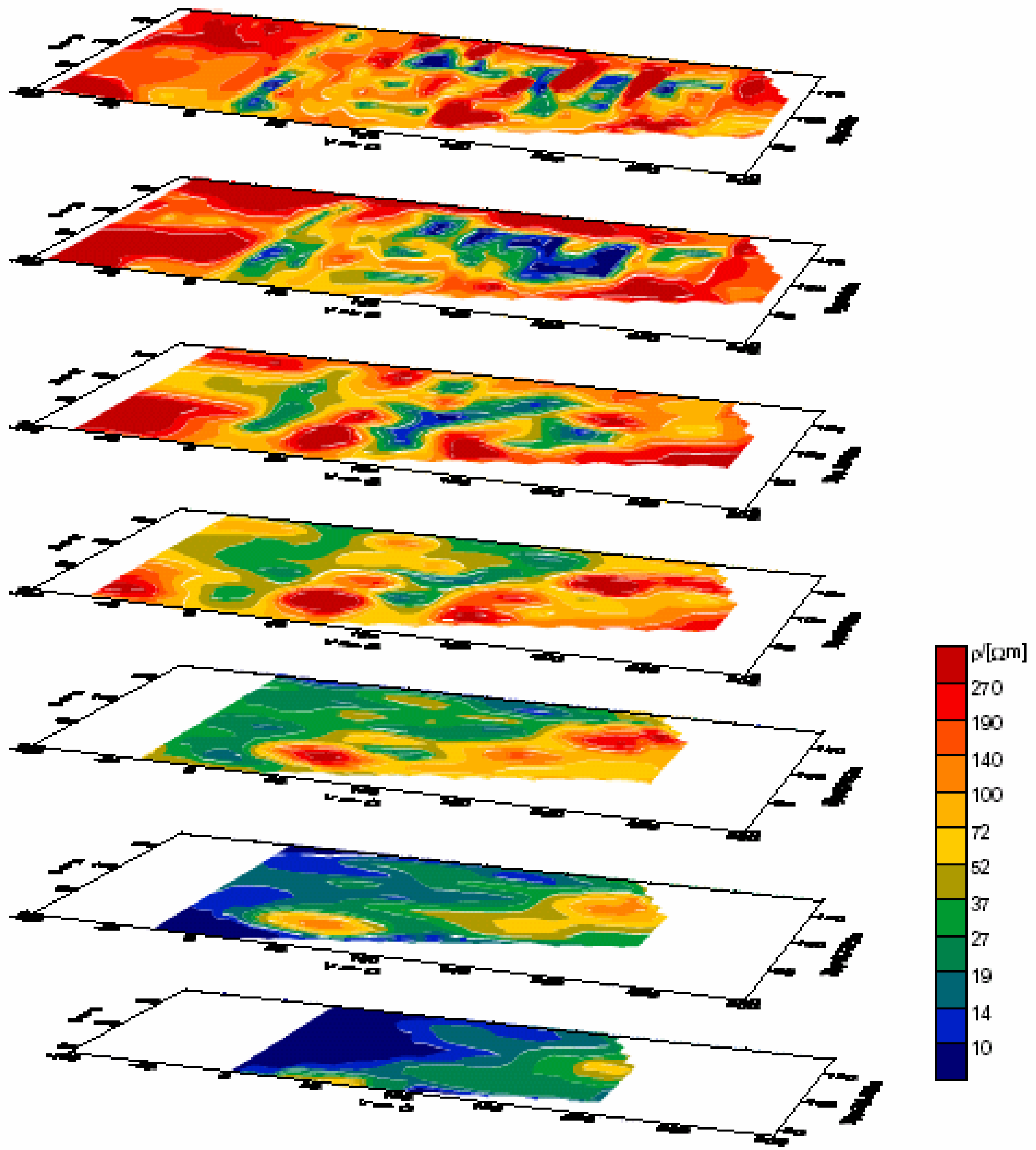

Figure 2. Inverted DC resistivity depth slices.

2.2 Electromagnetic methods (low frequency)

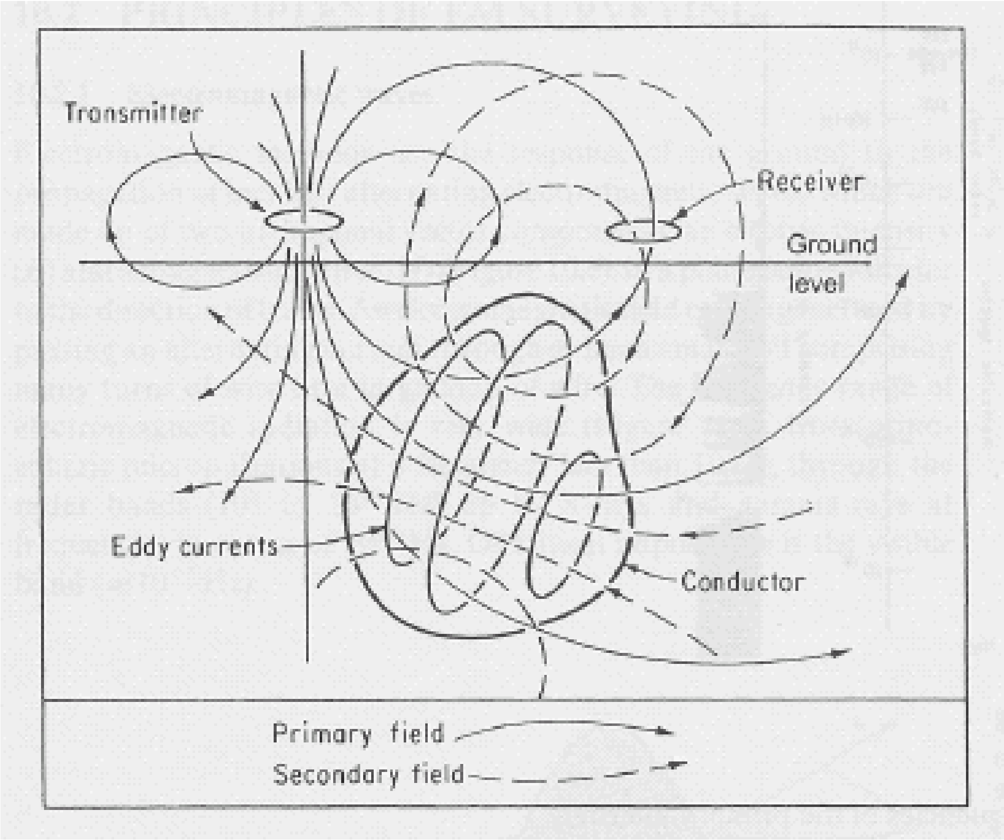

Generalized schematic of the EM surveying method. Both the primary and secondary magnetic fields are shown

EM instruments

TABLE 1. Exploration depths for EM34-3 at various intercoil spacings

Intercoil Spacing (meters)	Exploration Depth (meters)	
	Horizontal Dipoles	Vertical Dipoles
10	7.5	15
20	15	30
40	30	60

EM31

EM34

EM38

EM61

Example: Lernacken Sludge Deposit

The deposits at this site are known to consist of municipal waste, sludge containing industrial waste and large quantities of lime quarry waste. Heavily contaminated groundwater is present, in many cases reaching above regulatory levels. The major contaminants commonly found are organic antrophogenic matter and high levels of heavy metals. The bedrock in the region consists of tertiary limestone, which is overlain by glacial till reaching 5 - 15 meters.

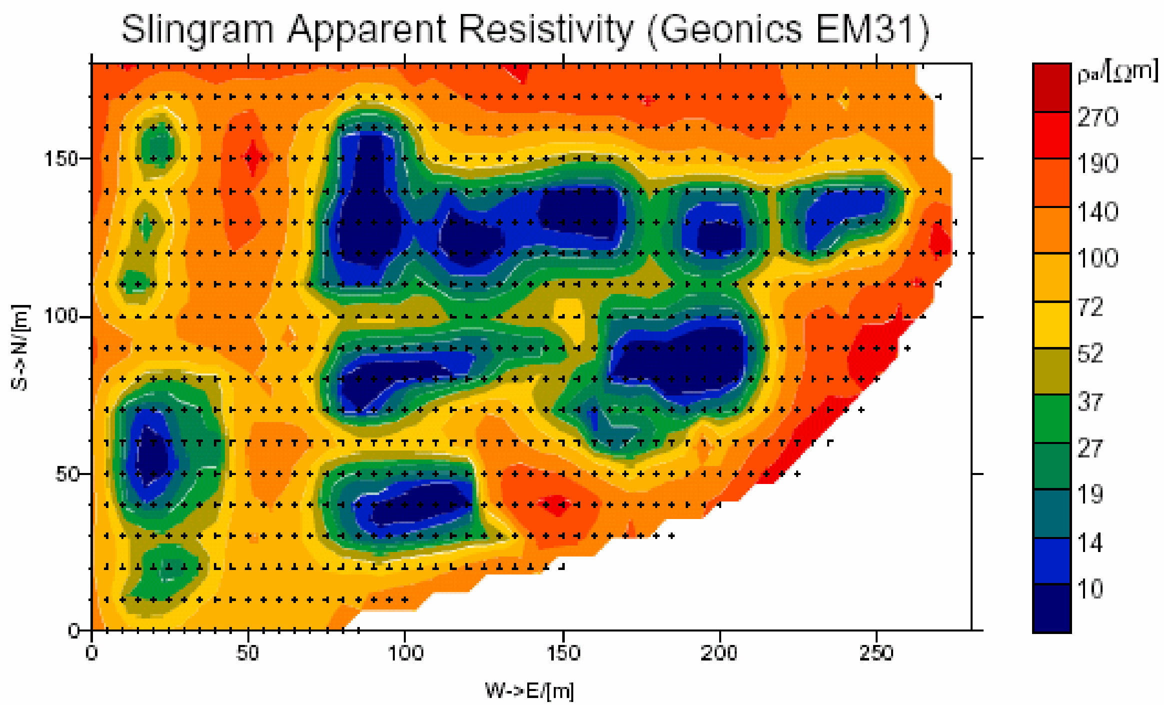

Figure 1. Slingram apparent resistivity.

Everglades National Park Site characterization (Fugro)

The main fresh water/ salt water interface is clearly mapped on all the coplanar resistivities as the red-orange to green-blue colour change. Other colour changes represent subtle variations in groundwater salinity, blue as fresh, red-purple as salt. The 56,000 Hz data is mapping the surface conductivity, and so shows lower conductivities as the fresh water rides on top of the salt water.

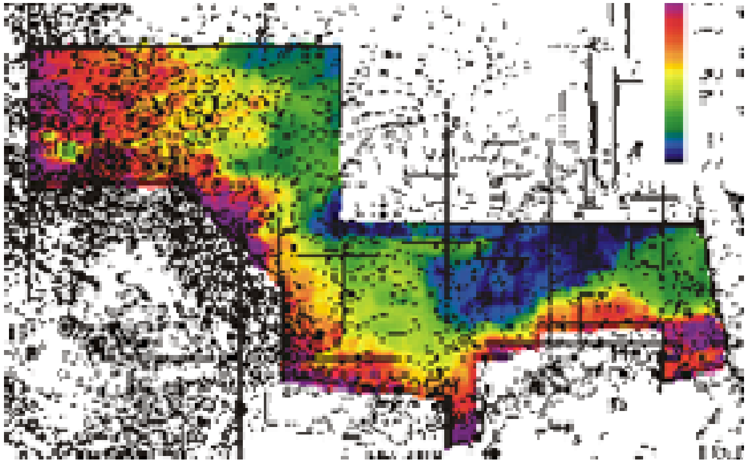

56000 Hz

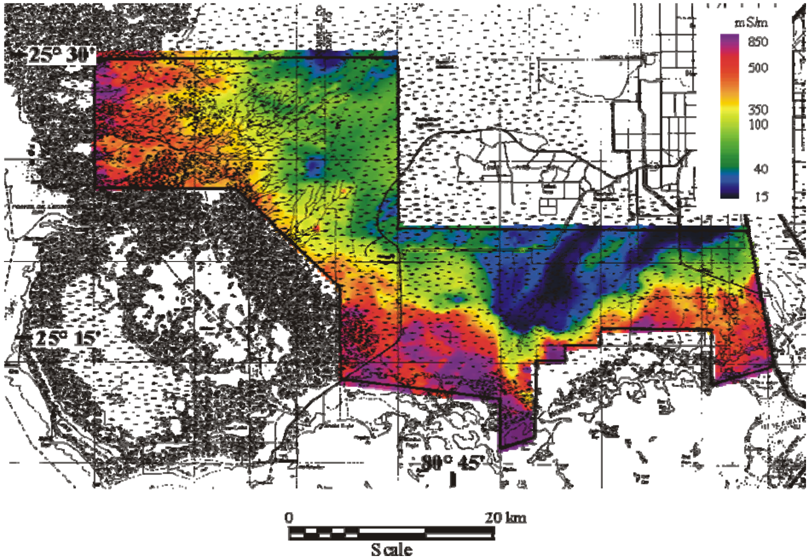

900 Hz

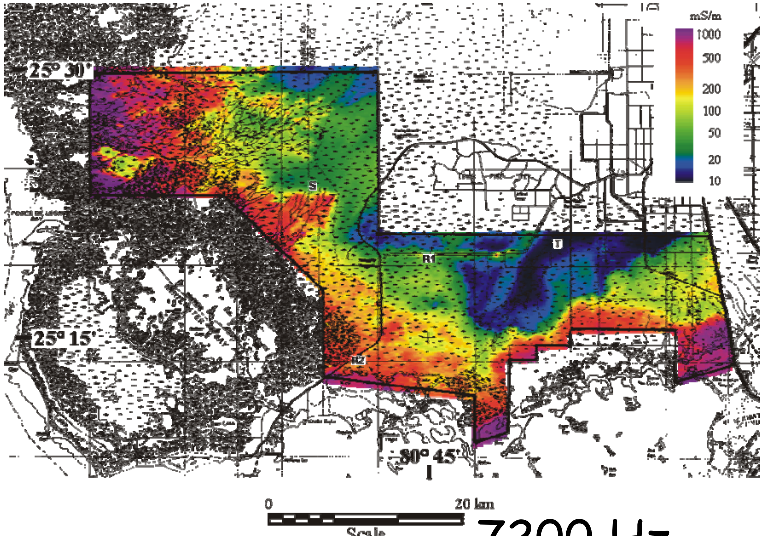

7200 Hz

4. Wave propagaating methods for imagery

4.1 GPR (géoradar) : Dielectric permittivity

4.1 Seismics (reflection, refraction)

Ground Penetrating Radar (GPR) : high resolution

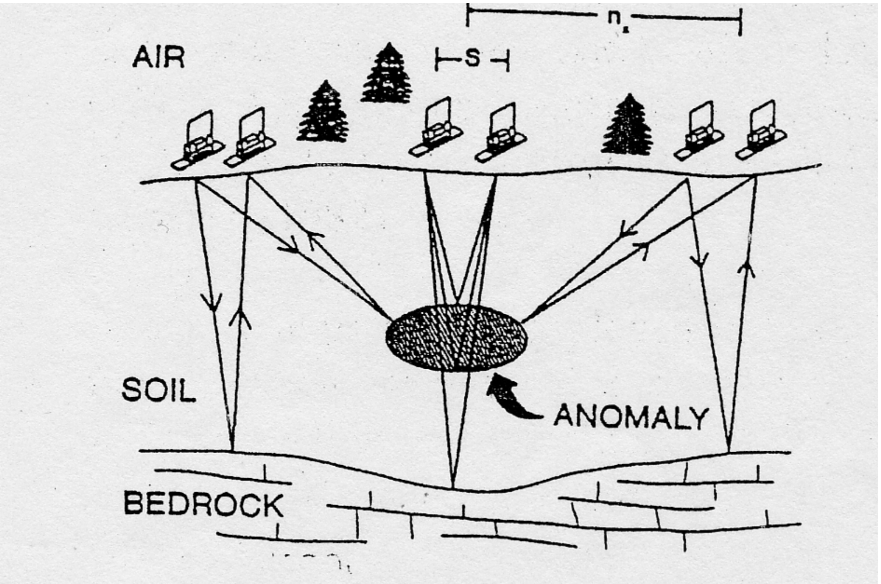

Figure 1.2: Schemaic illustration of common-offset single fold profiling.

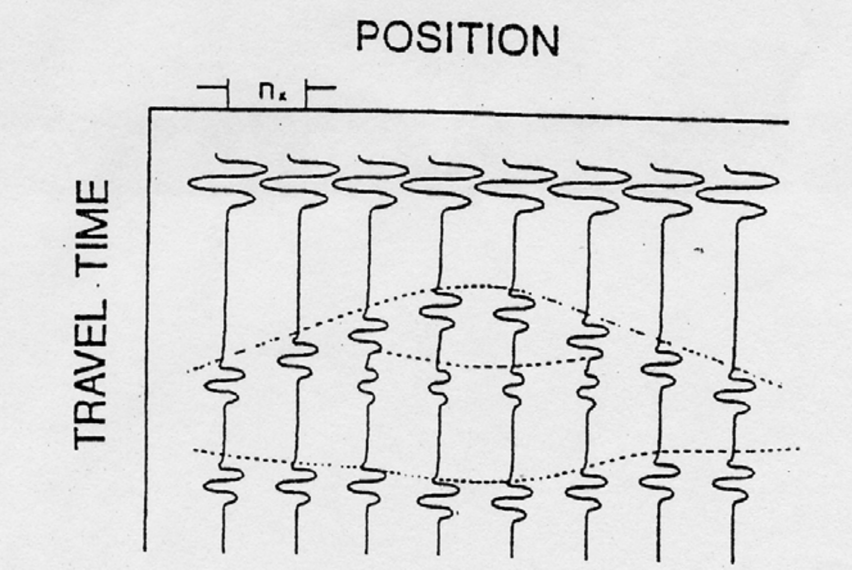

Figure 1.3: Format of a GPR reflection section with radar events shown for features depicted in Figure 1.2.

Only in resistive media !!!!!!!!!!!!!!!!

Radar equation

Maxwell equations can be reduced to (homogeneous, isotropic):

$$\nabla^2 \vec{E} = \mu\sigma \frac{\delta \vec{E}}{\delta t} + \mu\varepsilon \frac{\delta^2 \vec{E}}{\delta t^2}$$

(1) + (2)

μ : magnetic permeability ($\mu = \mu_0 \mu_r$)
σ :electrical conductivity
ε : dielectric permittivity ($\varepsilon = \varepsilon_0\ \varepsilon_r$)

(1) : diffusion term
(2) : propagation term

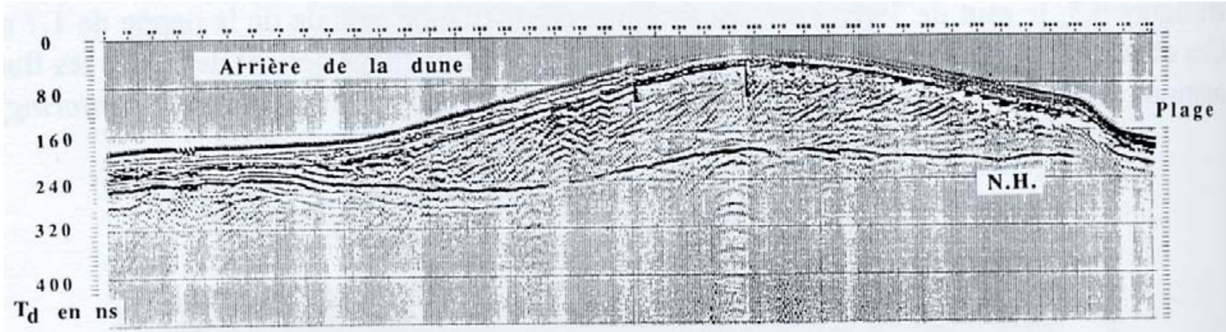

Figure 9.6 Image radar d'une dune côtière (Seignosse). N.H. : niveau hydrostatique (d'après Dubois, communication personnelle).

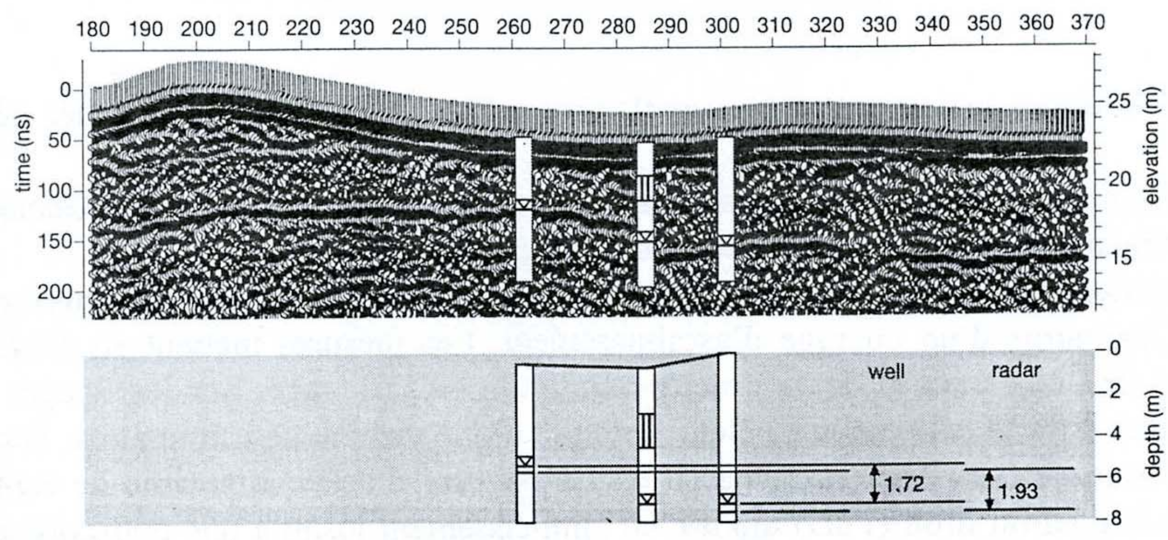

Figure 9.5 Détection du toit d'une nappe phréatique par radar de surface (d'après Van Overmeeren, 1994).

GPR data on a Peat bog –100 MHz

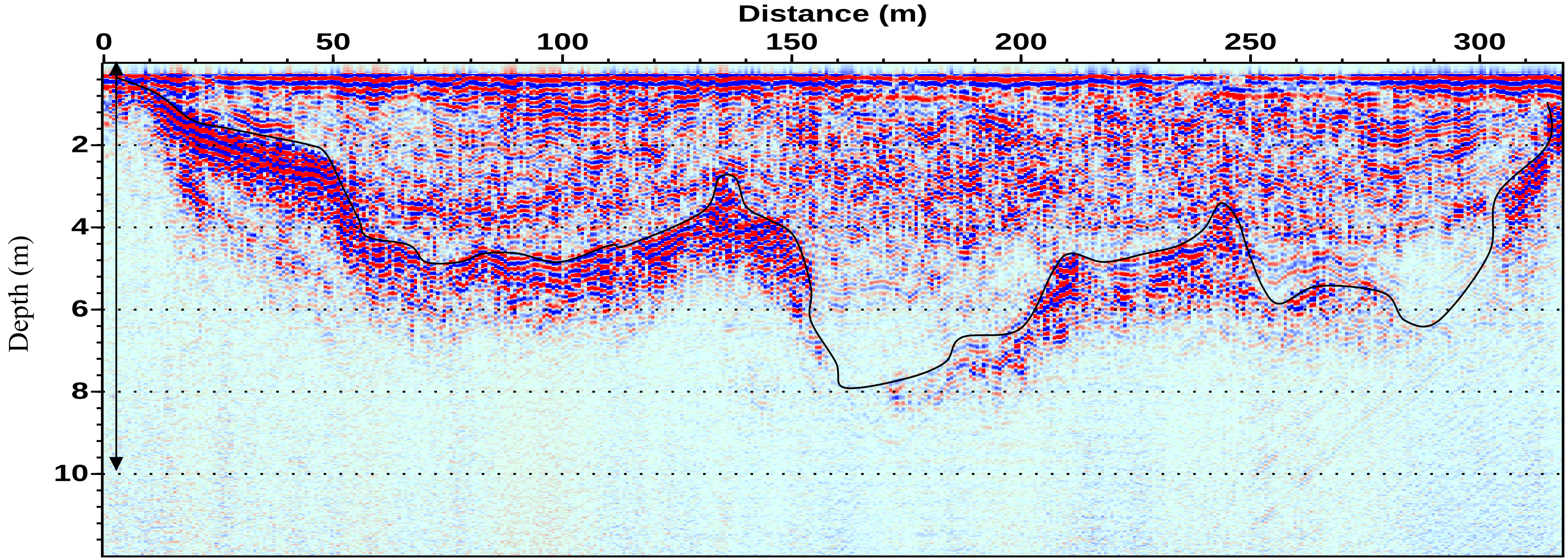

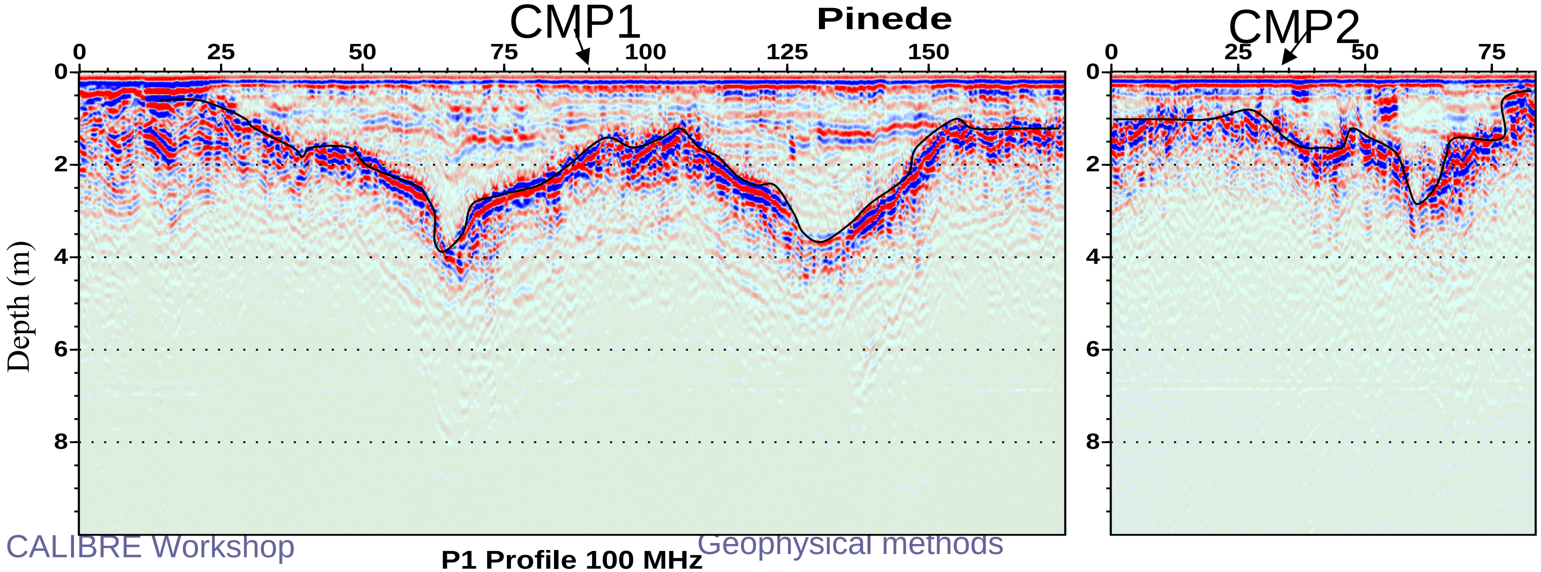

CMP acquisition (Annan)

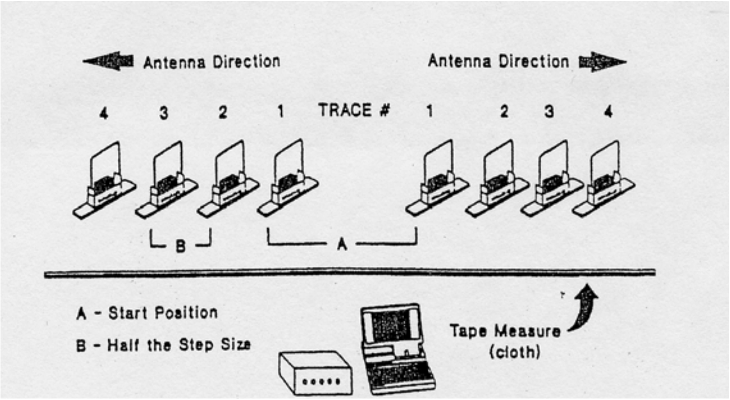

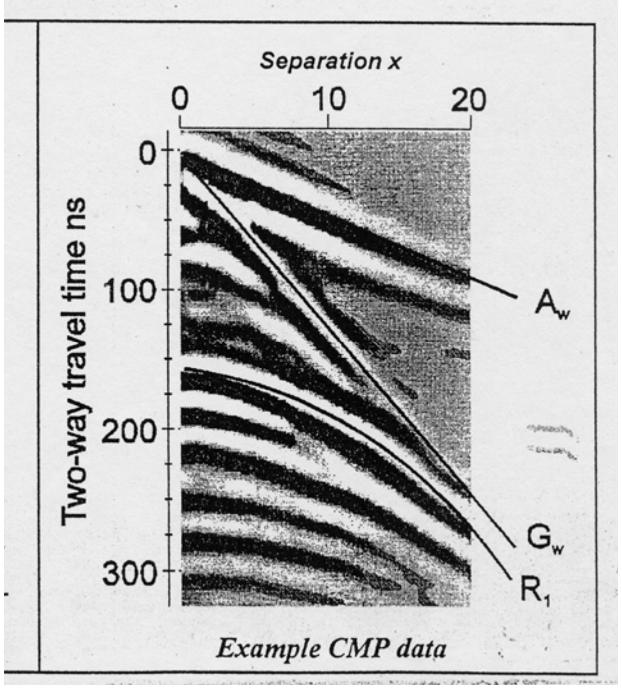

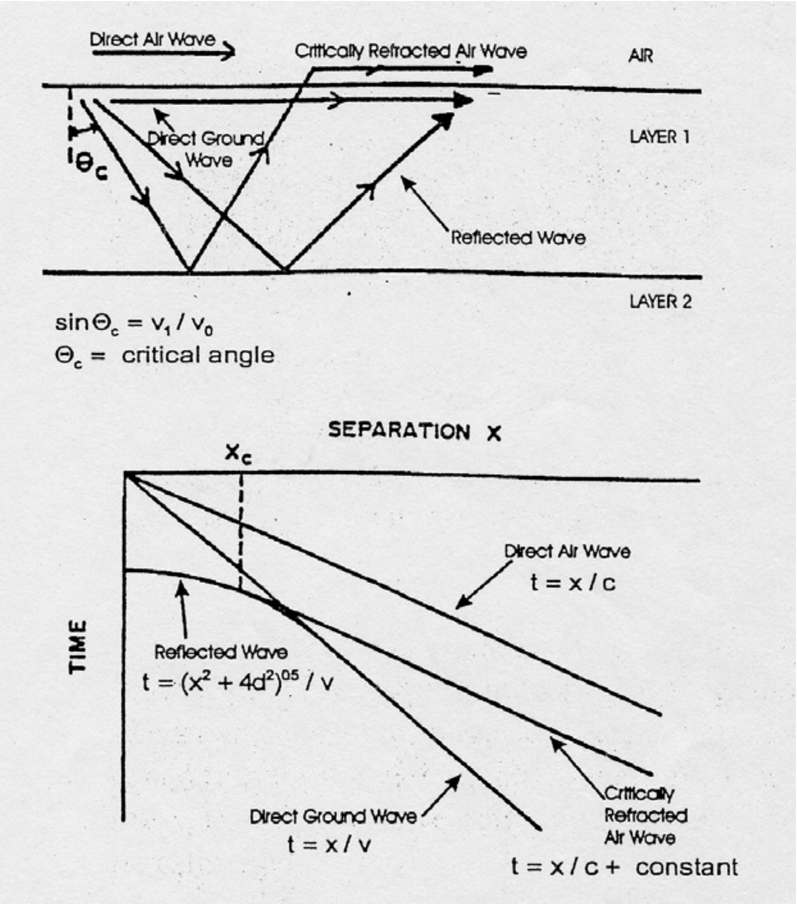

Figure 1.6: Illustration of CMP sounding ray paths and idealized event arrival-time versus antenna separation display.

Water content derived from GPR CMP data

CMP1

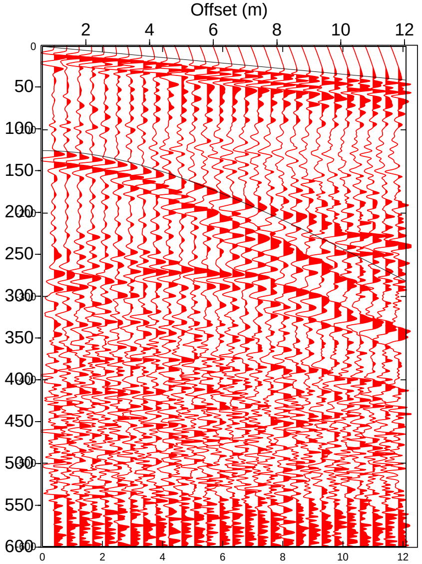

CMP2

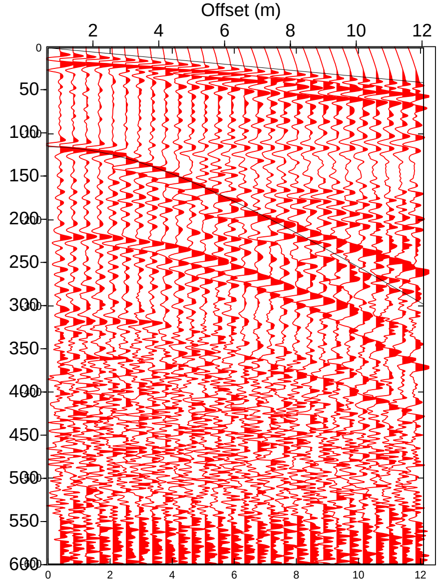

CMP8

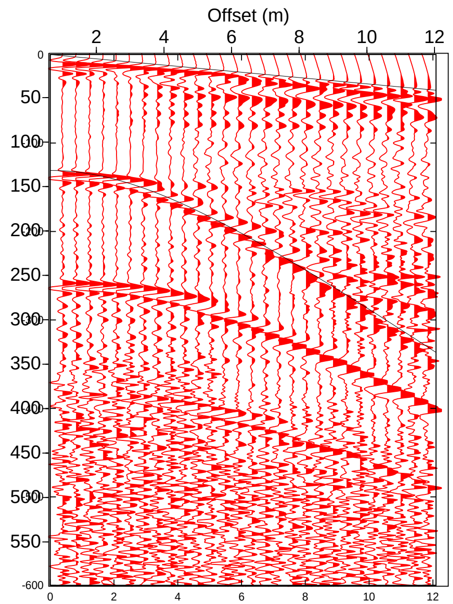

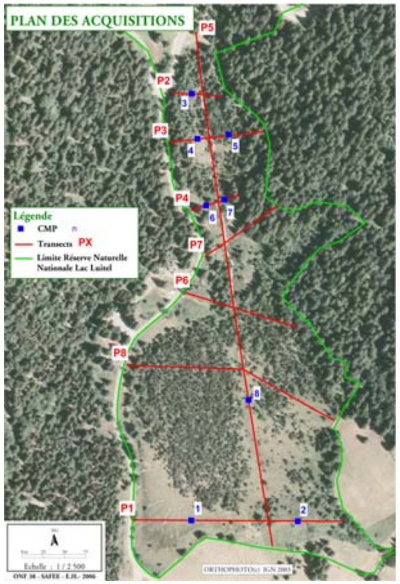

	Depth	Permit.	Water content (Topp et al)
CMP1	2.6 m	39	50 %
CMP2	2.2	46.5	55 %
CMP8	2.2 m	59.2	64 %

Studies of the unsaturated zone

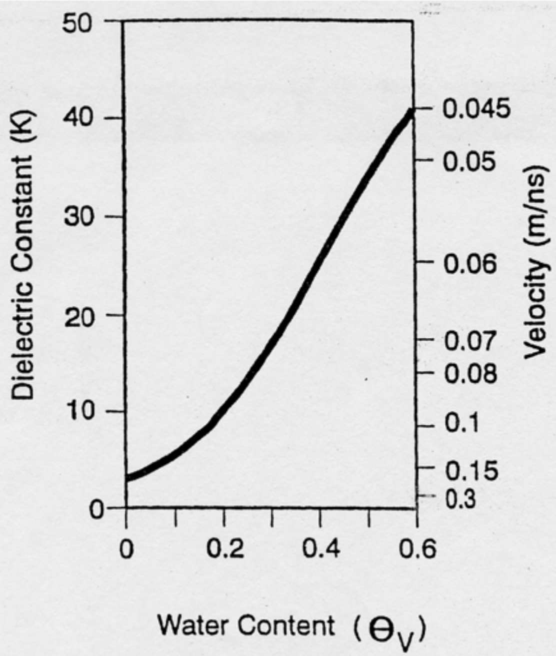

$$K_a = 3.03 + 9.3\,\theta_v + 146.0\,\theta_v^2 - 76.6\,\theta_v^3$$

$$\theta_v = -5.3\times10^{-2} + 2.92\times10^{-2}K_a - 5.5\times10^{-4}K_a^{\,2} + 4.3\times10^{-6}K_a^{\,3}$$

Figure 3.11: Variation of dielectric constant and velocity with water content.

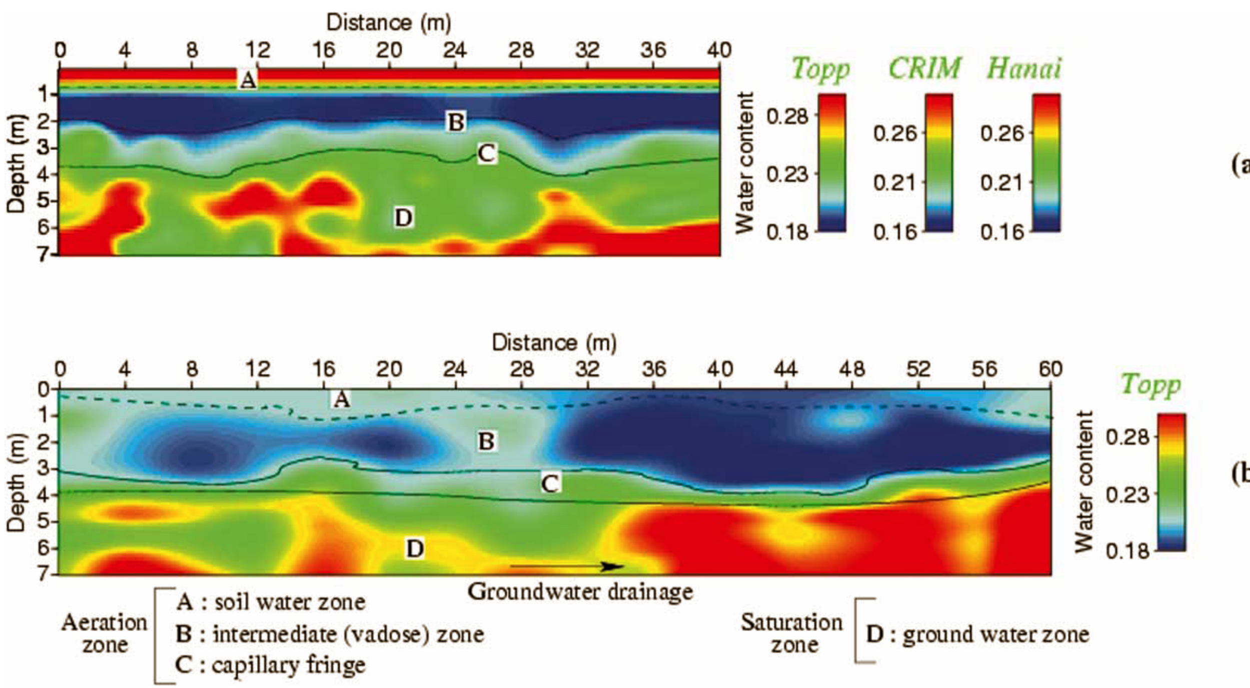

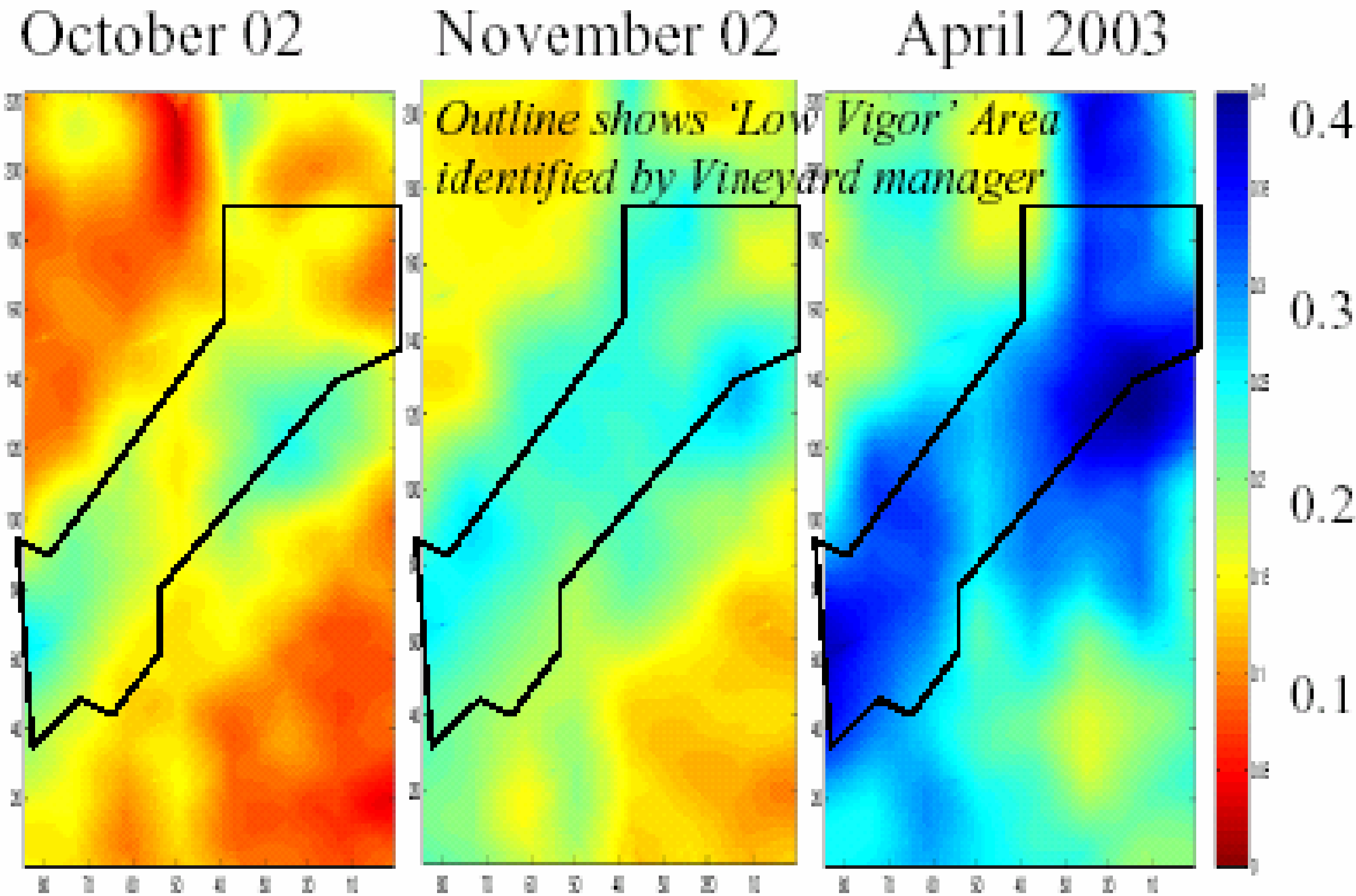

Figure 1 Average volumetric water content in the top 1.0-1.5m estimated over time using 100 MHz GPR reflection travel time data over 3-acre study block at the Dehlinger Vineyards (modified from [5]).

Ground Penetrating radar: glacier of Sarennes (avril 2006) :

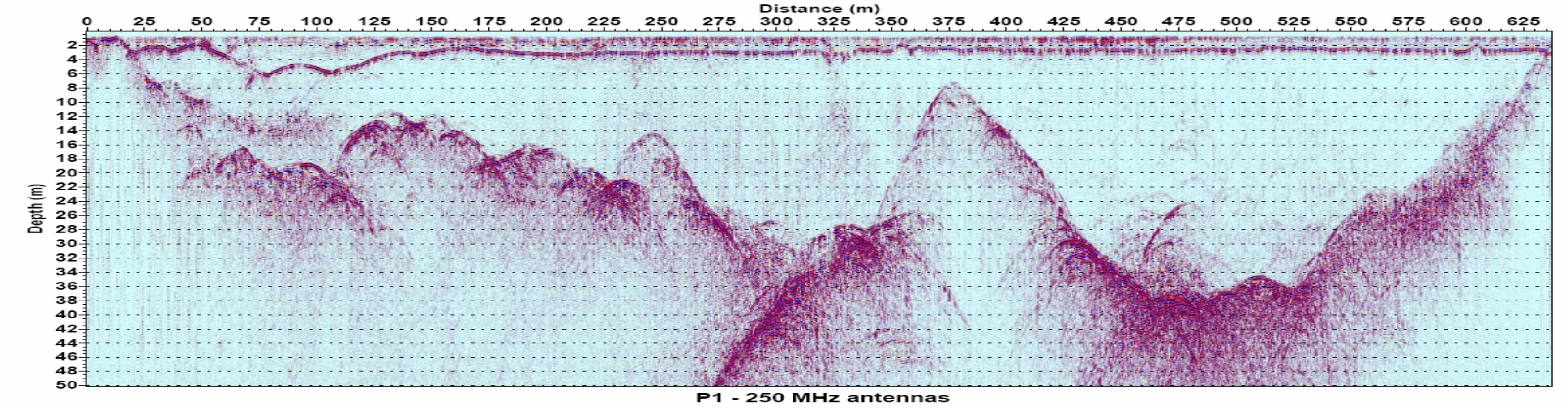

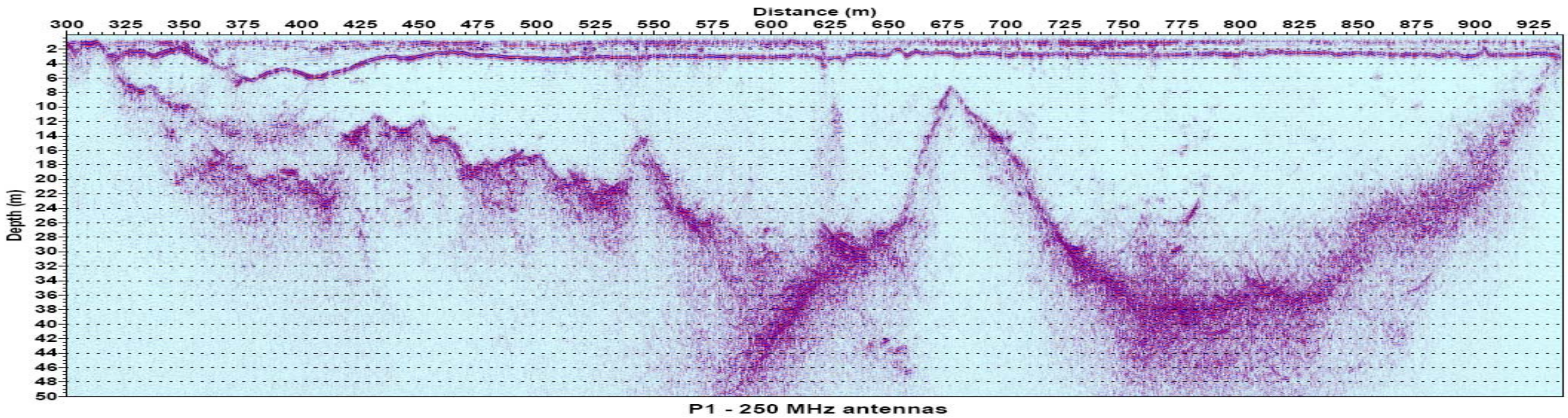

Géométrie des rais

Angle d'incidence

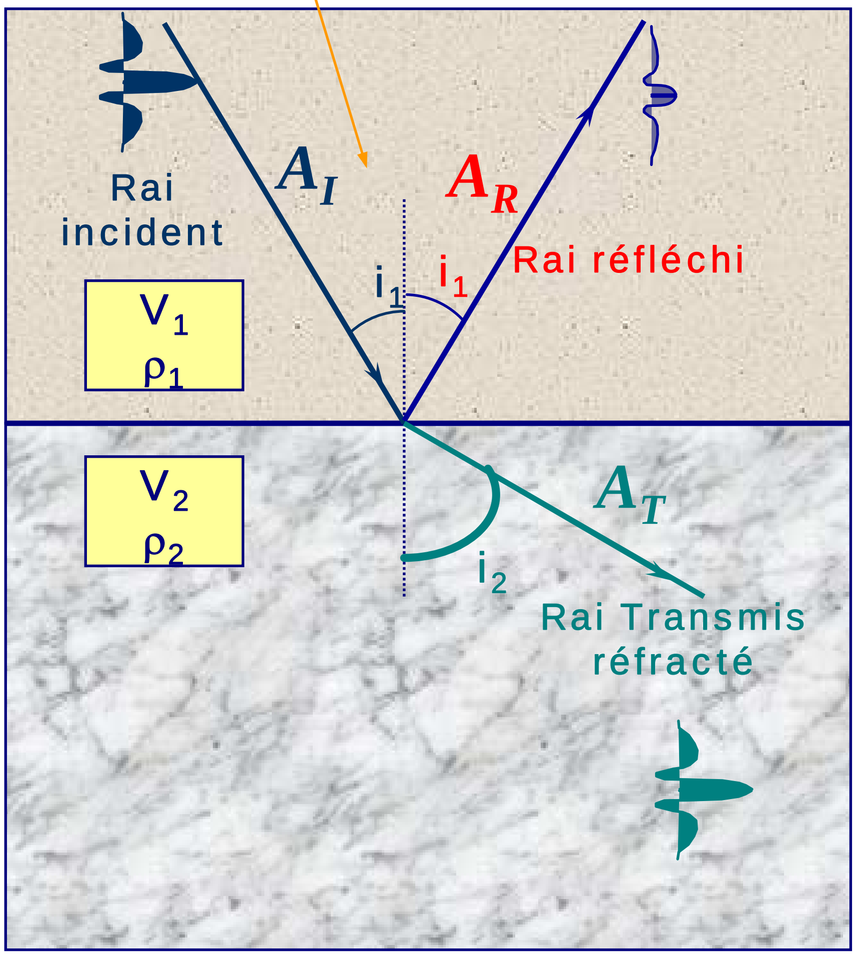

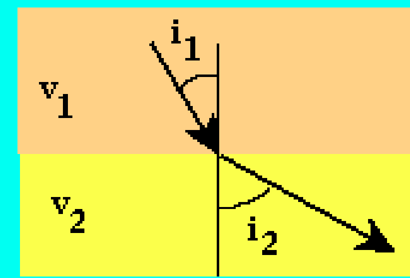

$$\frac{\sin i_1}{v_1} = \frac{\sin i_2}{v_2}$$

Loi de Snell-Descartes

Si V1 < V2

ρV = Impédance accoustique
ρ = Masse volumique
V = Vitesse

Classification of geophysical methods

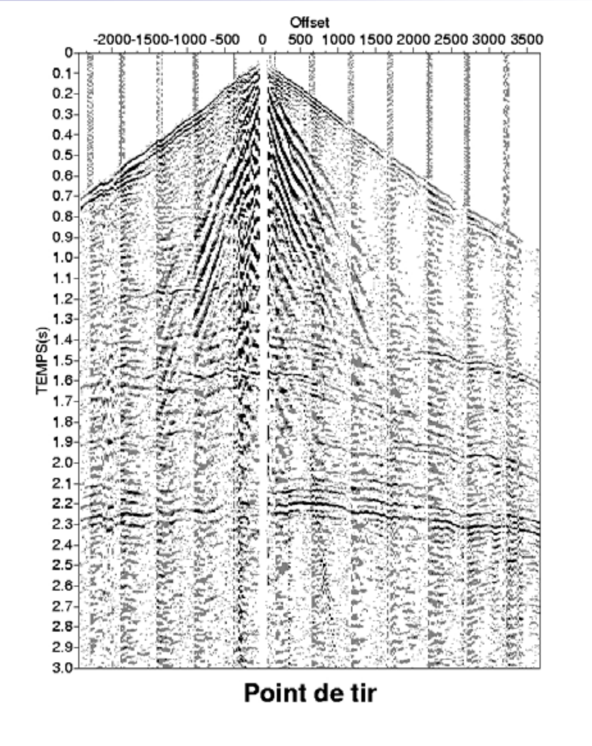

Seismic data

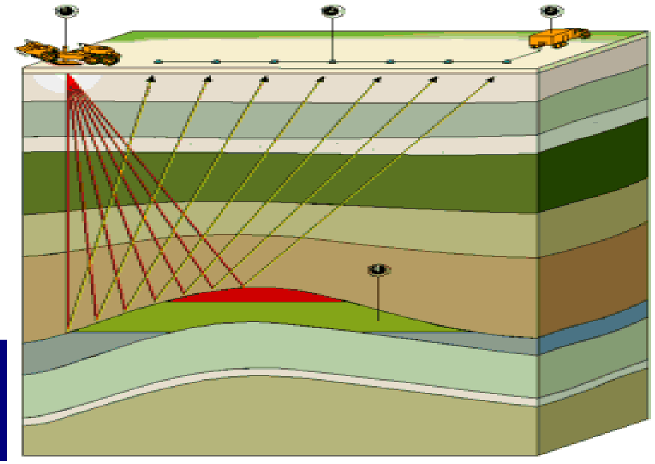

Acquisition of seismic data

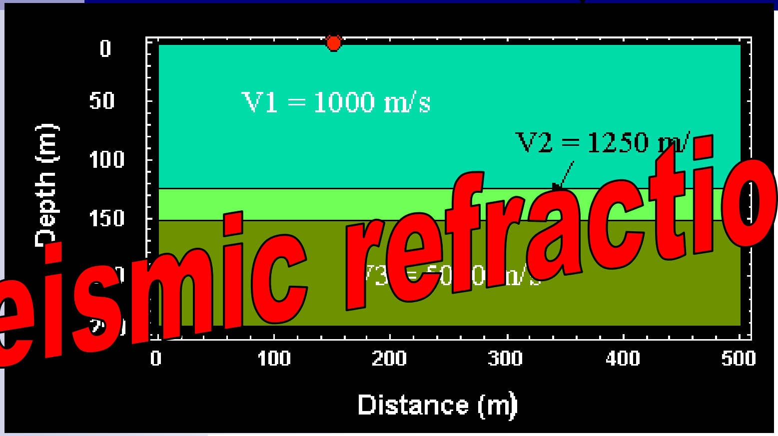

Modèle de terrain

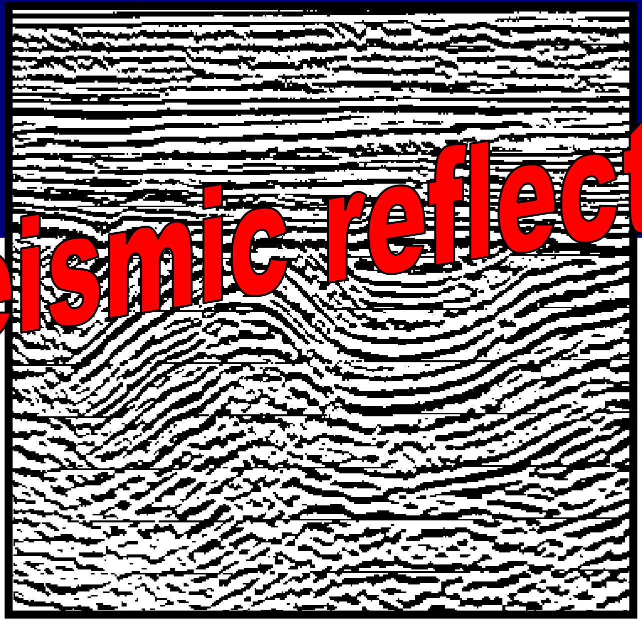

Section sismique

Seismic refraction

Seismic reflection

Depend on

- Matrix and structure of the stone
- Lithology
- Porosity
- Porefilling interstitial fluid
- Temperature
- Degree of compaction
- ………

Characteristics of P and S velocities

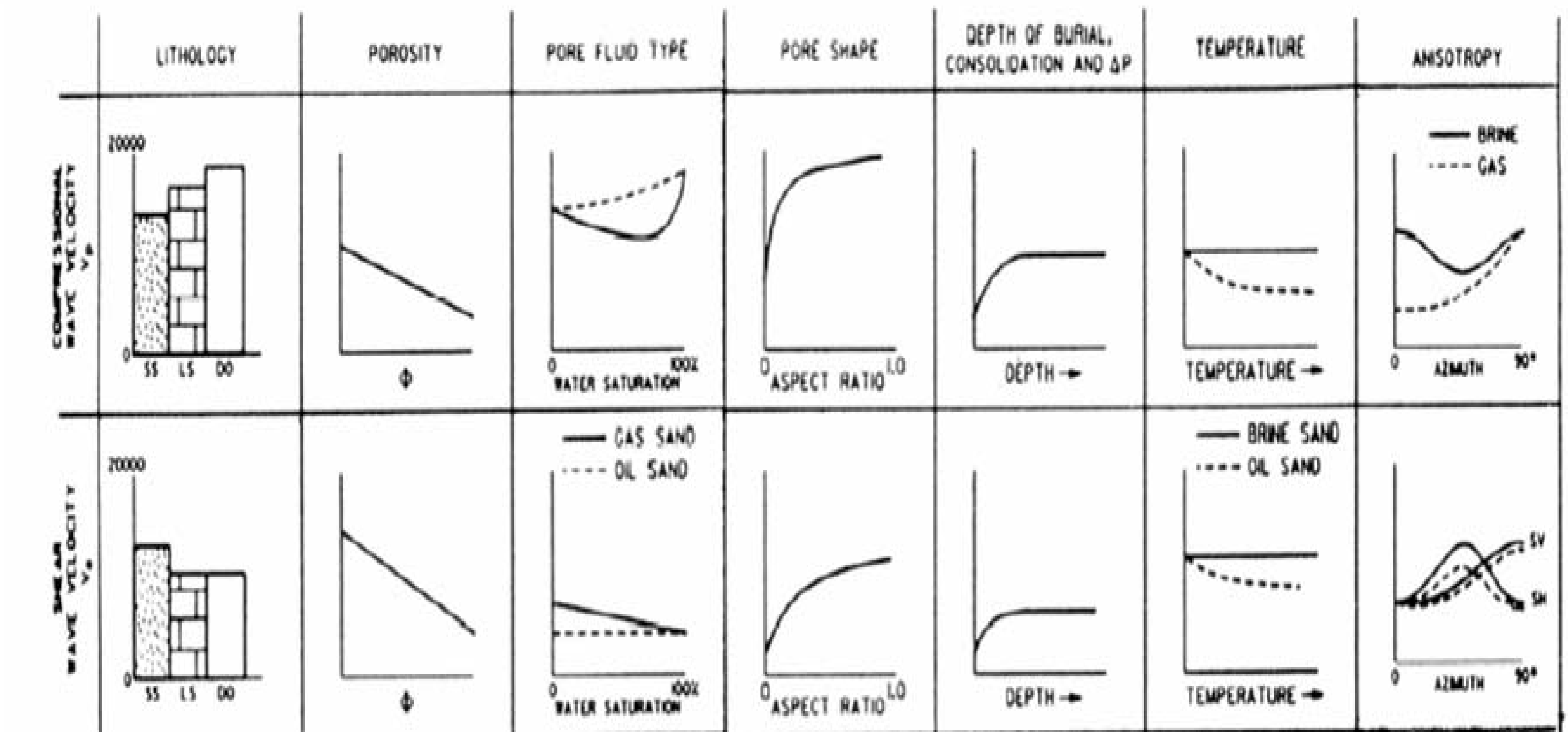

Examples
Groundwater

Objective:

Map subsurface location of aquifer for the purpose of drilling a well

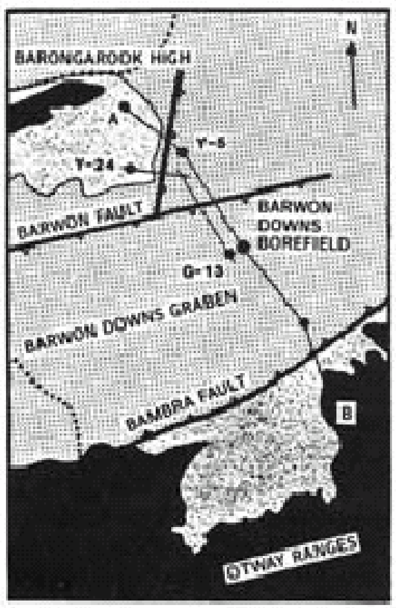

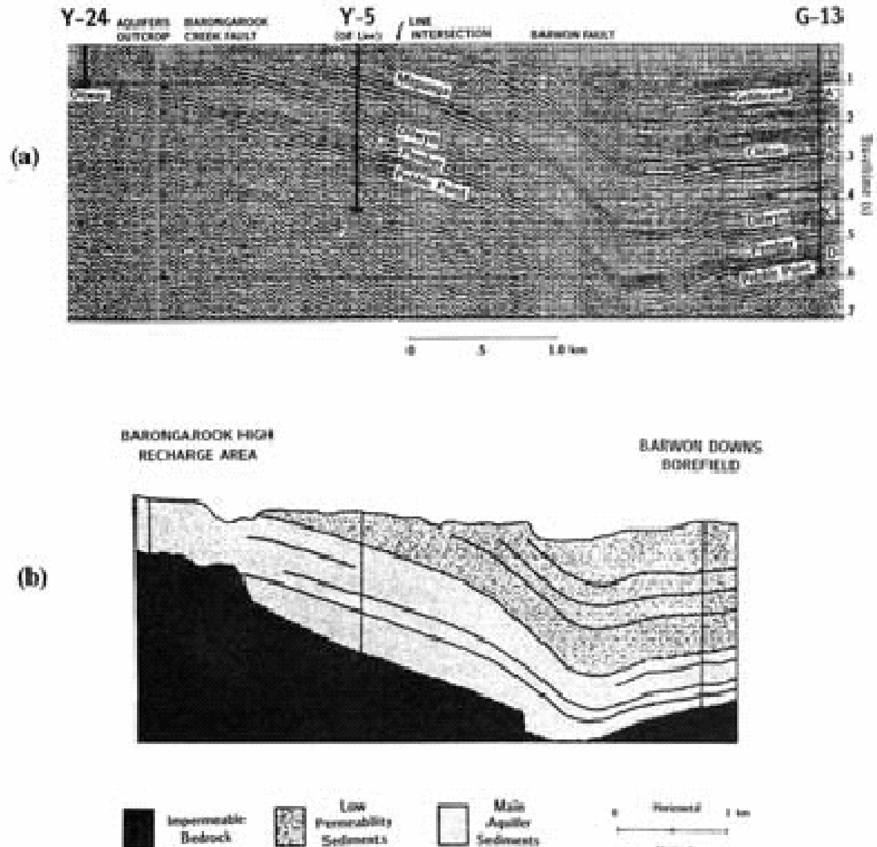

Fig. 4.29 (a) Seismic section below the survey line Y-24–G-13 (see location map, Fig. 4.28). Amplitude normalization and 3×vertical exaggeration used to emphasize structure in this section across the Barwon Downs graben. Main aquifer units are named below the line intersection; boreholes shown by thick solid lines. (b) Yeodene survey hydrogeological interpretation. The basal Tertiary aquifer system, confined between a calcareous aquitard cap and impermeable bedrock, is shown to be continuous between the Barongarook recharge area and the Barwon Downs extraction area. (After Geissler, 1989.)

Exemple de tomographie sismique

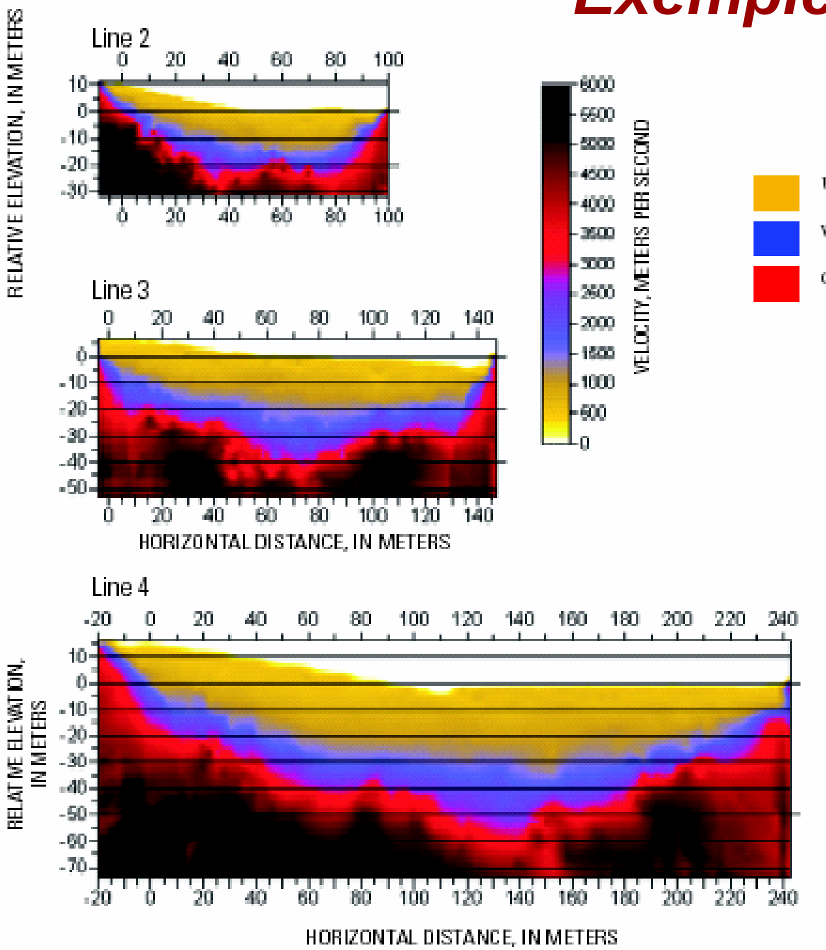

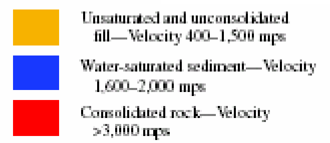

Figure 5. Velocity-depth images of seismic lines 1–4 at the same scale. Alluvium and bedrock distinguished by use of a color scale corresponding to common velocities of earth materials: dark yellow, unsaturated and unconsolidated fill (velocity 400–1,500 mps); blue, water-saturated sediment (velocity 1,600–2,000 mps); red, consolidated rock (velocity >3,000 mps).

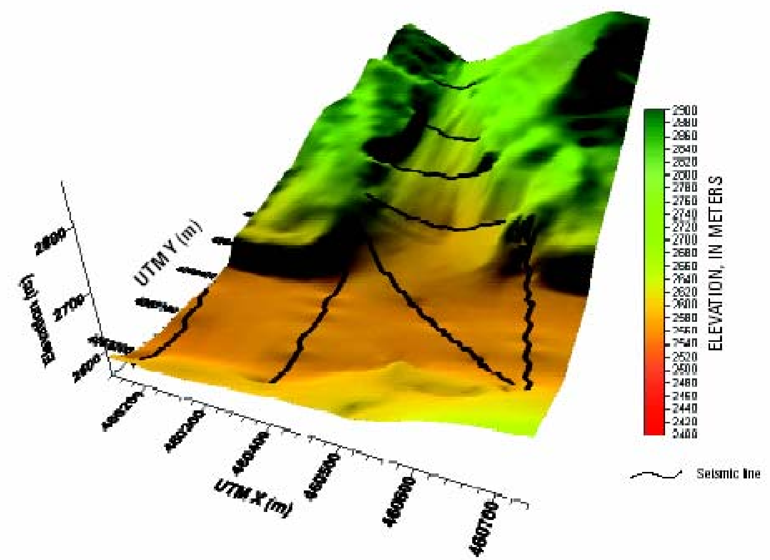

Figure 14. Configuration of water table near confluence of Straight Creek and Red River. Generated from surface-elevation values shown in figure 12 and from depth to the water table, defined by interpretation of seismic data. Dry alluvium graphically removed to reveal the water table. Seismic line locations cast to the nearest 10-m-grid locations.

2.3 Résonance Magnétique Protonique

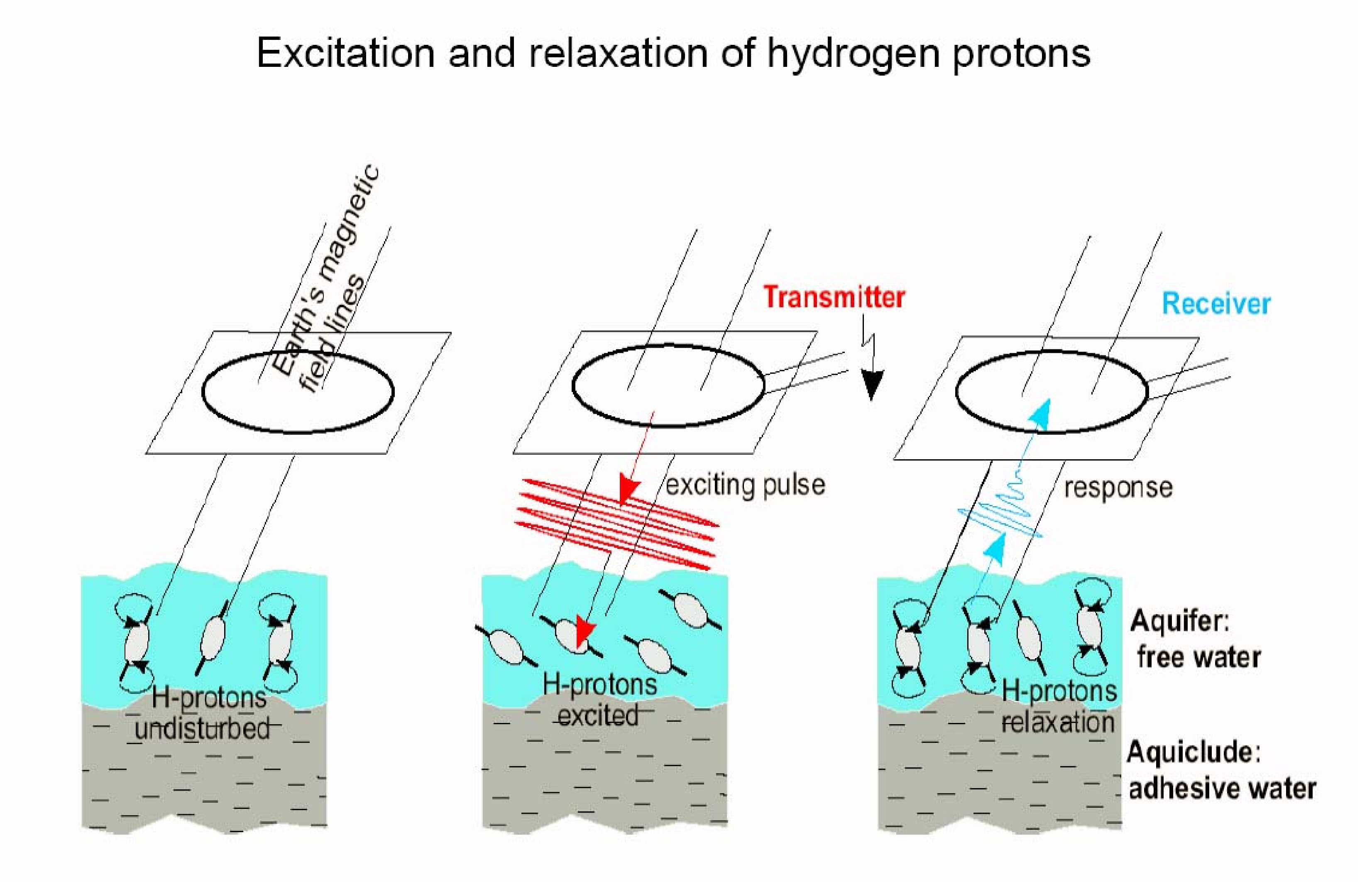

Basic principle of MRS measurements

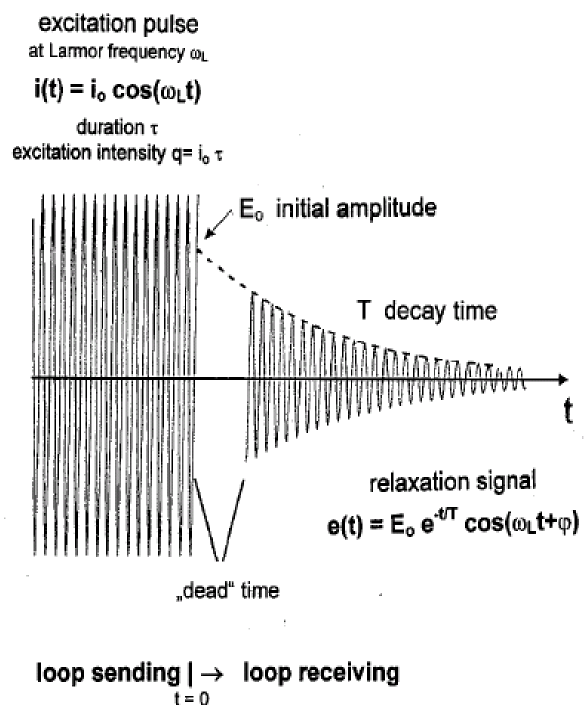

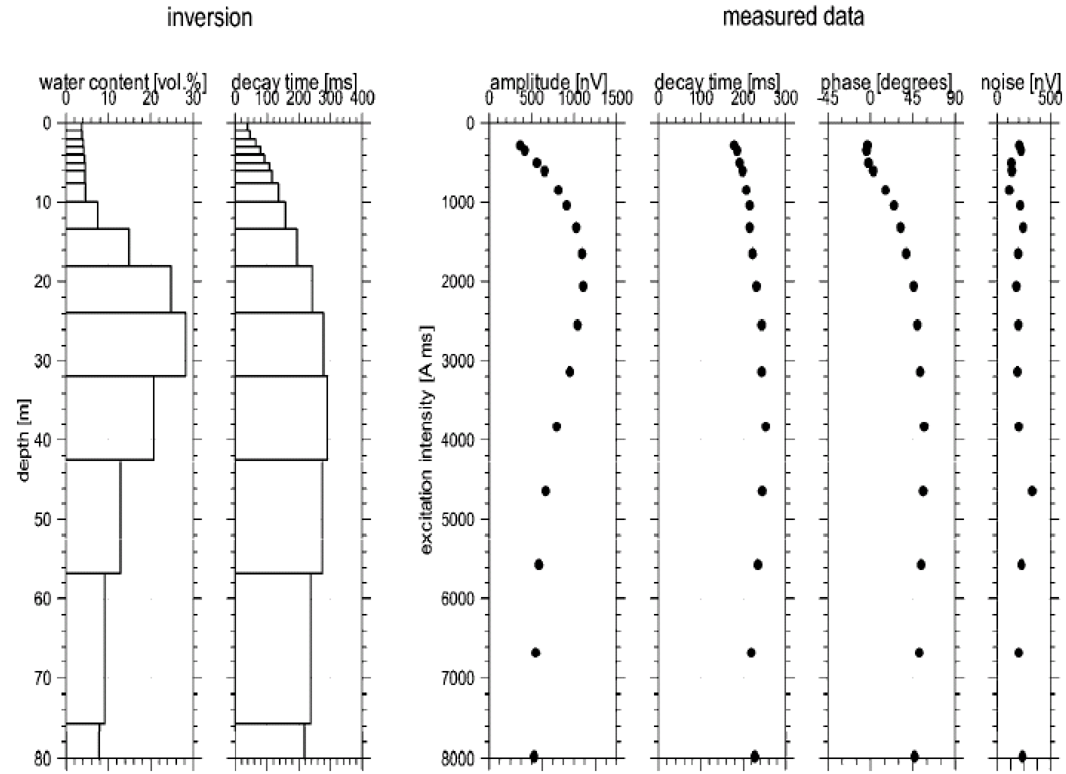

Measured quantity	Derived parameter
E_o Initial Amplitude	~ layer water content
T Decay Time	~ layer decay time ~ pore size ~ hydraulic permeability
φ Phase	~ layer electrical conductivity

PMR soundings in Andalusia (SPAIN)

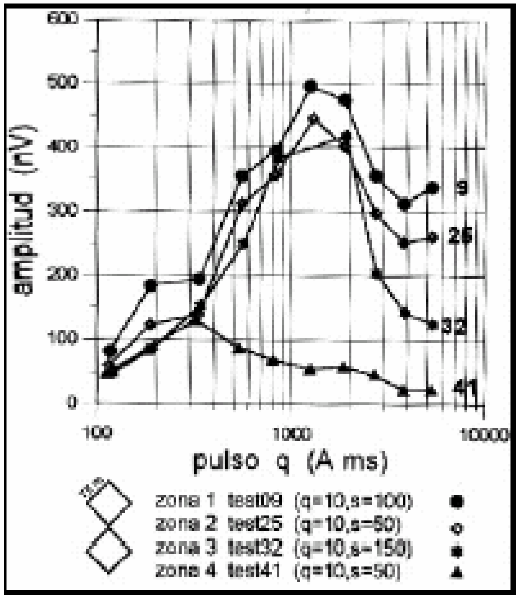

FIELD PMR SOUNDING CURVES

WITH EIGHT SHAPE LOOP

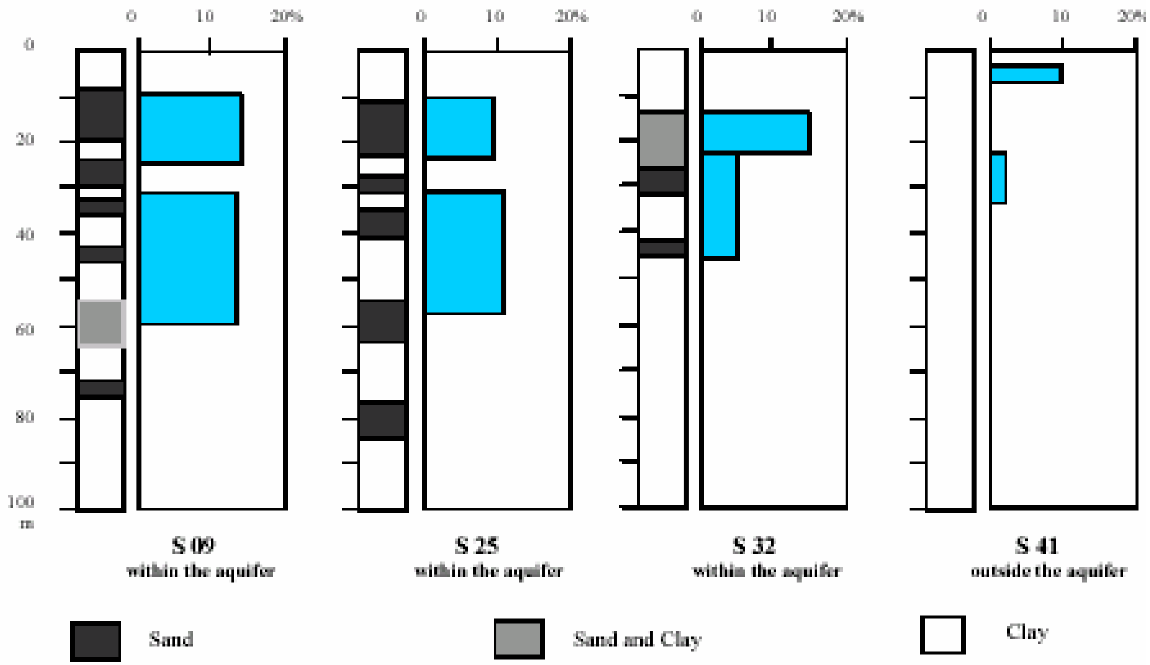

COMPARISON OF PMR SOUNDING INTERPRETATION

(WATER CONTENT VERSUS DEPTH) WITH DRILLHOLE GEOLOGICAL DATA

MRS and geoelectrics at test site 2

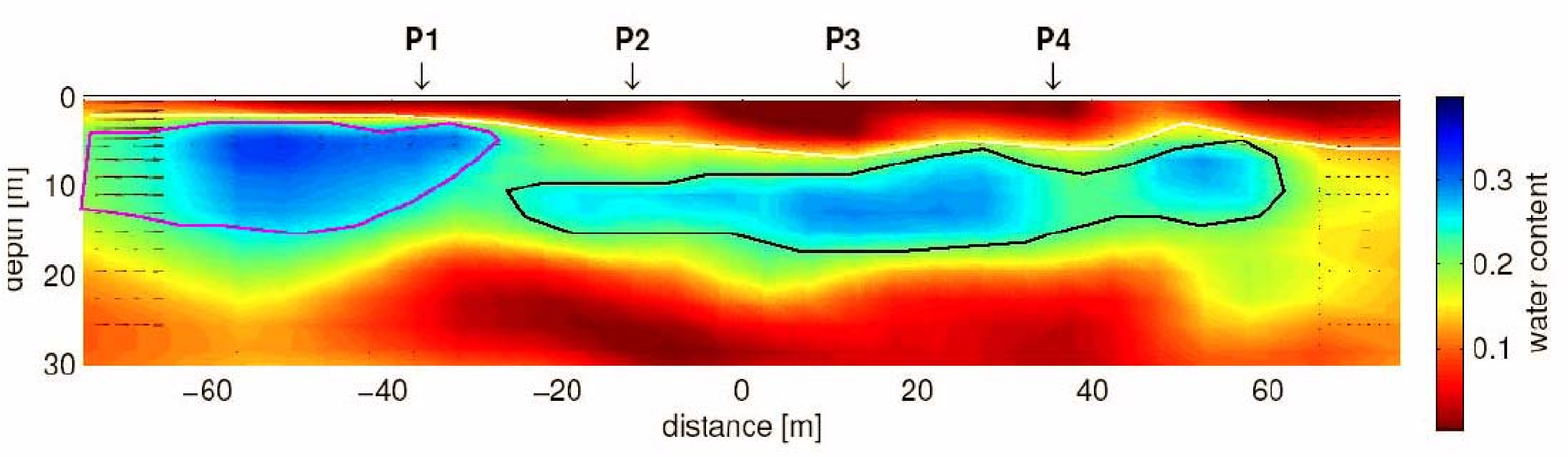


station C
(50 m)
station B
(30 m)
station A
(10 m)
water
level
sea level
W
E

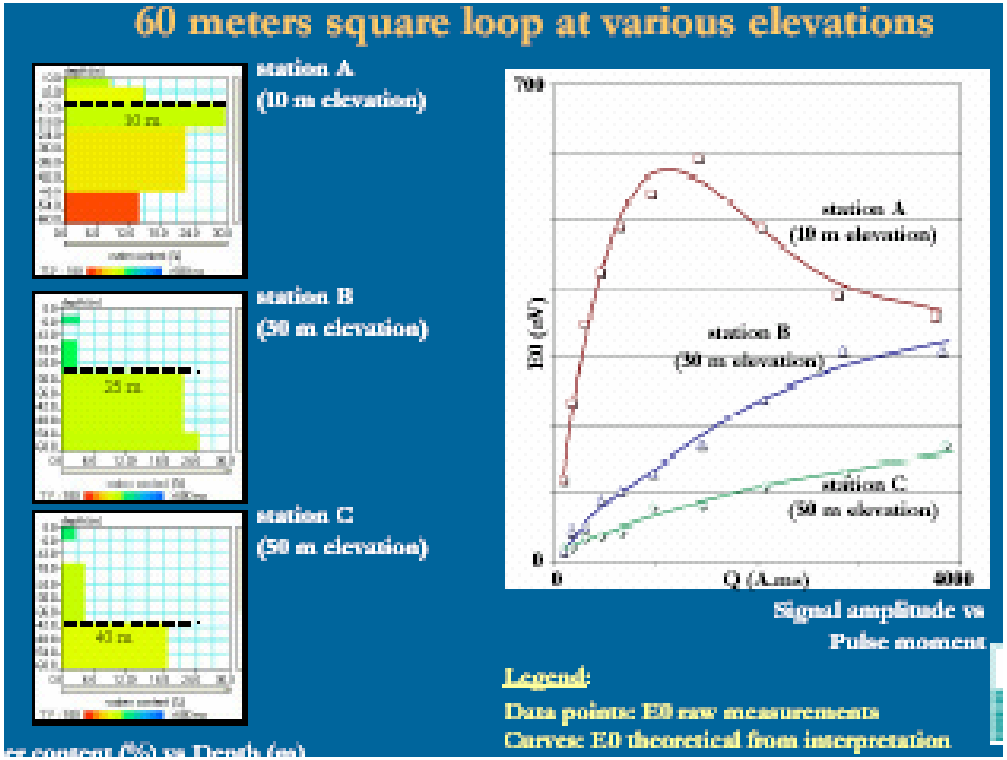
60 meters square loop at various elevations
station A
(10 m elevation)
10 m
station B
(30 m elevation)
25 m
station C
(50 m elevation)
40 m
er content (%) vs Depth (m)
700
0
E0 (nV)
Q (A.ms)
4000
station A
(10 m elevation)
station B
(30 m elevation)
station C
(50 m elevation)
Signal amplitude vs
Pulse moment
Legend:
Data points: E0 raw measurements
Curves: E0 theoretical from interpretation

3. Méthode électrique passive : PS

Prospection PS

Comment ça marche? *Principe (Mesure passive)*

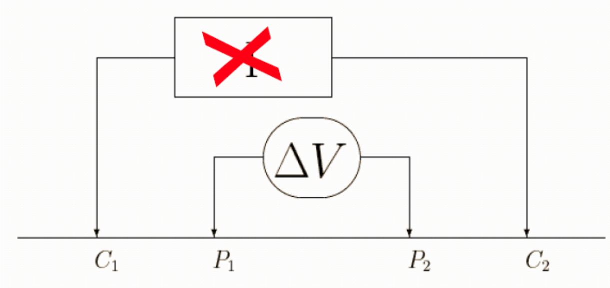

Données de potentiel
spontané (PS)
Mesurés près de la Surface

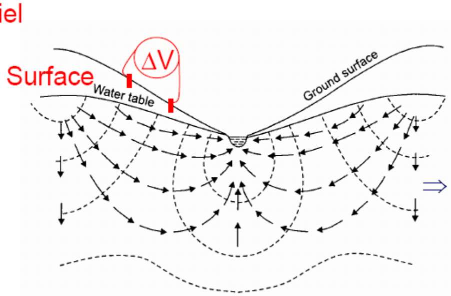

⇒ Modèles de Circulation
en profondeur

Table 8.2 Types of electrical potentials

Electrokinetic (electrofiltration) (electromechnical) (streaming)		Variable with time
Diffusion potential Liquid-junction	Electrochemical potentials	
Nernst potential (Shale)		
Mineral potential		Constant

Electrokinetic:

$$E_k = \frac{\varepsilon \mu C_E \delta P}{4\pi\eta}$$

where: ε, μ and η are the dielectric constant, resistivity and dynamic viscosity of the electrolyte respectively; δP is the pressure difference; and C_E is the electrofiltration coupling coefficient.

Prospection PS

Imagerie et interprétation *inversion*

Genetic algorithm and pumping test application

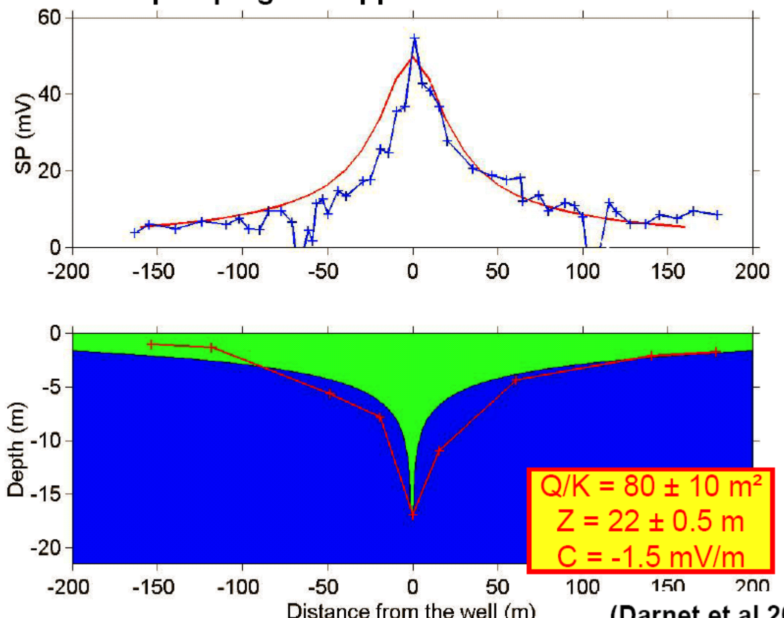

(Darnet et al 2003 / GRI

Use full inverse modelling including pumping and soil parameters C, Q/K,…

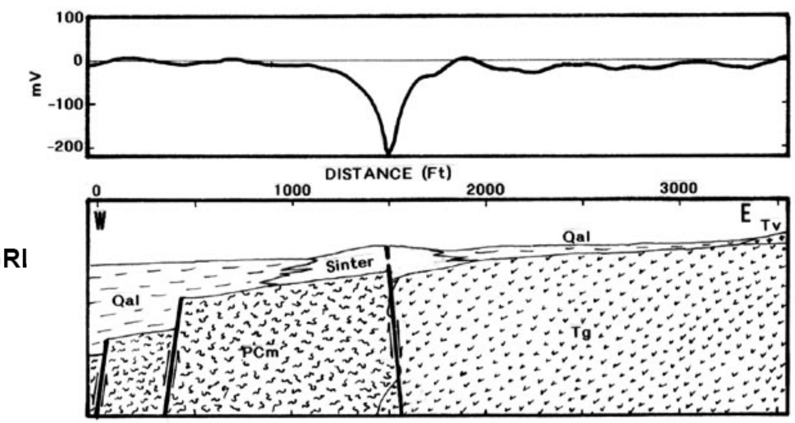

ROOSEVELT HOT SPRINGS KGRA

Resistivity Imaging and Spontaneous Potential (SP) Survey for Dam Investigation

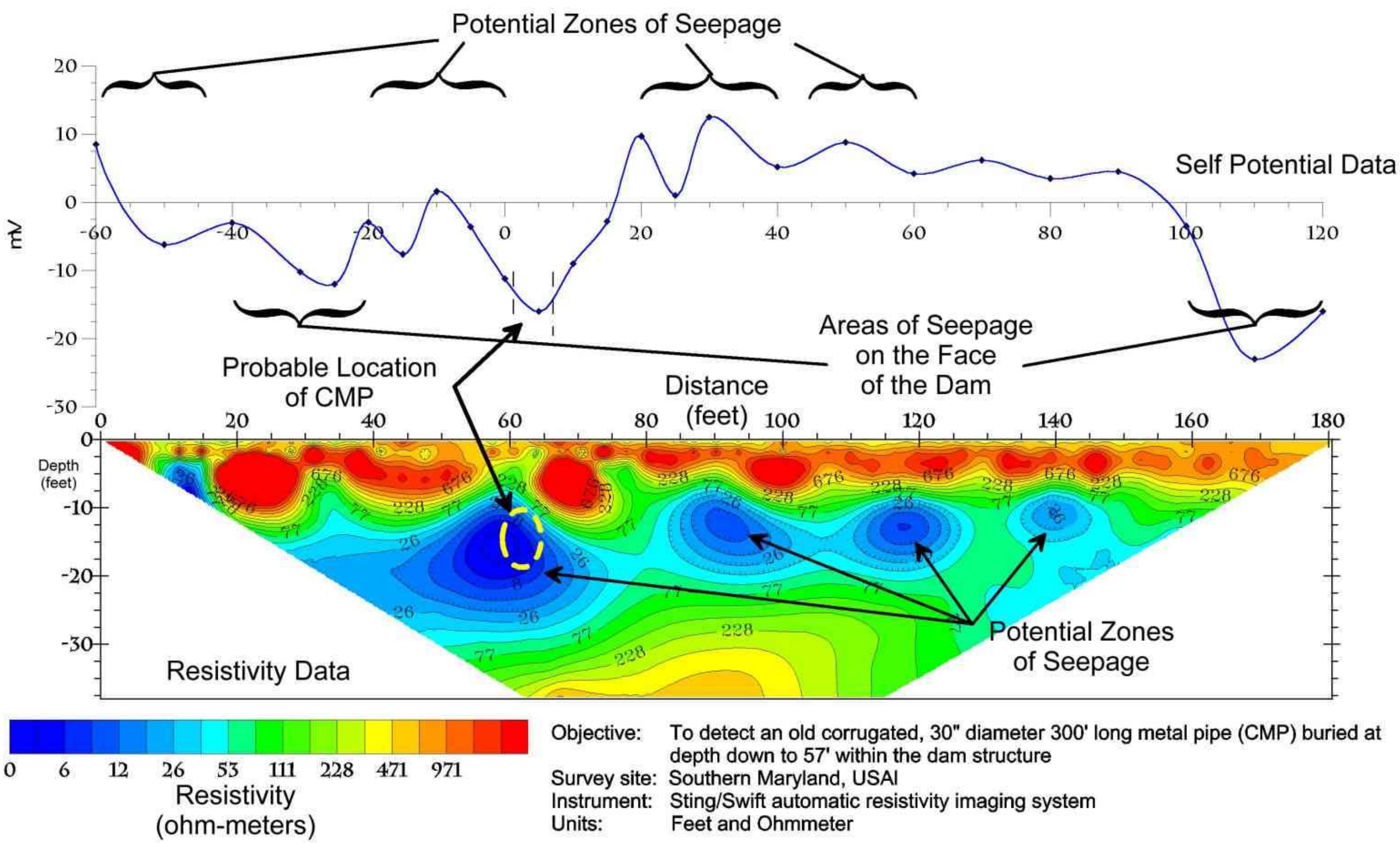

Objective:	To detect an old corrugated, 30" diameter 300' long metal pipe (CMP) buried at depth down to 57' within the dam structure
Survey site:	Southern Maryland, USAI
Instrument:	Sting/Swift automatic resistivity imaging system
Units:	Feet and Ohmmeter

Courtesy of
Schnabel Engineering

A number of geophysical methods such as magnetometer, gravimeter, spontanious potential (SP) and resistivity imaging were used. The SP and resistivity methods were the most successful at locating the pipe at depth. A total of 30 holes were drilled and only 6 of them missed the pipe.

AGI Advanced Geosciences, Inc.

Tel: +1 (512) 335-3338
Fax: +1 (512) 258-9958
E-mail sales@agiusa.com
Web site http://www.agiusa.com